International Review of Financial Analysis 73 (2021) 101599

Contents lists available at ScienceDirect

International Review of Financial Analysis

journal homepage: www.elsevier.com/locate/irfa

Stock returns, quantile autocorrelation, and volatility forecasting

Yixiu Zhao [a,*], Vineet Upreti [b], Yuzhi Cai [c]

[a] School of Economics and Management, Harbin Engineering University, Harbin, China
[b] School of Management, Swansea University, Swansea, United Kingdom
[c] School of Management, Swansea University, Swansea, United Kingdom

ARTICLE INFO

Keywords:
Quantile autoregression
Stock returns
Volatility forecasting
Volatility asymmetry

ABSTRACT

We examine stock return autocorrelation at various quantiles of the returns' distribution and use it to forecast stock return volatility. Our empirical results show that the strength of the autoregression varies across the quantiles of the returns' distribution in terms of both magnitude and persistence. Specifically, the autoregression order and magnitude of the coefficients is lower in the left tail in comparison with the right tail. Additionally, we show that the quantile autoregressive (QAR) framework proposed in this study improves out-of-sample volatility forecasting performance compared to the generalised autoregressive conditional heteroscedasticity (GARCH)-type models and other quantile-based models. We also observe greater outperformance in QAR estimates during periods of financial turmoil. Moreover, the QAR method also explains the stylized 'leverage effect' associated with asset returns in the presence of volatility asymmetry.

1. Introduction

Research on volatility forecasting is abundant. Volatility forecasting is broadly applicable in financial markets, including, but not limited to, risk management (Engle & Patton, 2001), option pricing (Andersen & Bollerslev, 1998), and monetary policy (Bernanke & Gertler, 2000). One of the key strands running through the extant literature on volatility modelling is the use of models from the autoregressive conditional heteroscedasticity (ARCH) and generalised autoregressive conditional heteroscedasticity (GARCH) time series model family; see Poon and Granger (2003) for a review. Multiple extensions of these models have been proposed to capture additional stylised facts observed in volatility series, such as volatility asymmetry (Engle & Ng, 1993; Glosten, Jagannathan, & Runkle, 1993), and structural changes in the dynamics of volatility documented in studies like Ardia et al. (2019) and Wang, Shrestha, and Sun (2019). Recently, greater attention has been given to quantile-based techniques for analysing realized volatility. For example, Taylor (2005) and Huang (2012) directly apply the quantile regression model to generate volatility forecasts and their studies show that the out-of-sample performance of their models is superior to traditional GARCH-type models. Choi and Shin (2018) also develop a parametric model for quantile forecasts of realized volatilities. Similar to GARCH models, quantile-based models contain all information of financial series that is captured in GARCH models (Baur & Dimpfl, 2017).

In this paper, we propose a novel quantile-based method to generate volatility forecasts. There are several important motivations for using this type of approach. The first motivation is that the existing studies, such as GARCH-type models, assume the innovation term follows a parametric distribution, e.g. the normal distribution. In other words, the volatility forecasts produced by these models are based on the assumption that the shape of the conditional distribution is fixed over time. However, as suggested in prior studies, the return and volatility distribution of assets is most often heterogeneous (Bouri, Jalkh, & Roubaud, 2019), and if there is variation in the shape of the distribution over time, these models can generate inaccurate volatility forecasts (Taylor, 2005). Quantile regression, pioneered by Koenker and Bassett Jr (1978), is immune to this parametric model problem. Moreover, prior studies suggest that quantile regressions can provide greater insight into the interdependence of variables across the whole distribution. For example, Troster, Bouri, and Roubaud (2019) suggest that the mean-based model is inappropriate to analyse the casual relationship between financial assets in the presence of tail-dependence or nonlinear causal relationships. Their studies uncover the heterogeneity in the flights-to-safety effect with the implied volatilities by employing a quantile regression analysis. Han, Linton, Oka, and &Whang Y. J. (2016) use the cross-quantilogram to detect predictability from stock variance to excess stock return, and their results exhibit a more complete relationship between risk and return. Similarly, by employing quantile

* Corresponding author.
E-mail addresses: zhaoyixiu@hrbeu.edu.cn (Y. Zhao), v.upreti@swansea.ac.uk (V. Upreti), y.cai@swansea.ac.uk (Y. Cai).

https://doi.org/10.1016/j.irfa.2020.101599
Received 18 March 2020; Received in revised form 8 August 2020; Accepted 1 October 2020
Available online 9 October 2020

regression, Bouri et al. (2019) discover the differences in the dependence of volatilities of commodity prices and sovereign CDS spreads across different quantiles. Baur, Dimpfl, and Jung (2012) documents that the lower and upper quantiles of past returns exhibit different dependence behaviours. In this study, we propose a quantile autoregressive (QAR) method that accommodates autocorrelation in stock returns at various quantile levels in order to generate volatility forecasts. Due to its ability to deal with temporal variation in returns' distributions, the volatility forecasts produced via this method are likely to be more accurate.

The use of quantile regression techniques has been increasing steadily in the field of finance. For example, these techniques are used to model capital asset pricing (Barnes & Hughes, 2002); return forecasts and optimal portfolio construction (Ma & Pohlman, 2008); hedge fund strategy implementation (Meligkotsidou, Vrontos, & Vrontos, 2009); economic activity and financial development (Demirgüç-Kunt, Feyen, & Levine, 2012); identifying the determinants of credit default swap spreads (Pires, Pereira, & Martins, 2015); interest rate sensitivity (Ferrando, Ferrer, & Jareño, 2017); oil volatility shocks (Xiao, Hu, Ouyang, & Wen, 2019); as well as in studying reaction of stock markets to international economic policy uncertainty and geopolitical risks (Kannadhasan & Das, 2020). However, studies focused on applying quantile-based methods for volatility forecasting are still evolving, and our paper adds to this stream of literature.

We start by investigating the dependence pattern in stock returns over a wide range of quantiles of the returns' distribution via the estimation and analysis of the sample quantile partial autoregressive function (QPACF) of a number of stock index returns following the method proposed by Li, Li, and Tsai (2015). Specifically, we consider five stock indices, namely, the CAC 40, DAX 30, FTSE 100, NIKKEI 225, and S&P 500 at daily frequencies. This paper uses quantile levels ranging from 0.1 to 0.9, which increase in steps of 0.05, to examine the dependence pattern for stock returns at various quantiles of the returns' distribution. The full sample spans the period from March 2000 to February 2019 and contains more than 4600 observations for each return series. Our sample has been chosen such that the financial crisis of 2008/9 occurs in the middle of the sample, providing us with approximately the same number of observations to analyse before and after the crisis. In order to evaluate the forecasting performance, we divide the entire sample into two sets, i.e. training and testing datasets. Then the training dataset is used to estimate the sample QPACF, and the testing dataset is used to evaluate out-of-sample performance.

Our QPACF analysis shows that, at the median (the middle quantile) of the returns' distribution, the impact from past returns is relatively weak, as no significant and persistent dependence pattern in stock returns is detected. In contrast, the analyses conducted for the lower and upper quantiles reveal persistent dependence patterns for stock returns. Additionally, our results show that the lower quantiles of the current returns' distribution are positively dependent on past returns, while the upper quantiles produce a negative dependence. We then go on to specify the QAR model based on the dependence pattern obtained using the QPACF analysis. Next, we compare the forecasting performance of the QAR specification with those of other forecasting models. A broad mix of benchmark models are used for comparison, namely, Markov switching (MS) and Markov switching Glosten-Jagannathan-Runkle (MS-GJR) versions of GARCH(1,1) models with different distribution assumptions, and variants of the quantile-based models of Taylor (2005) and Huang (2012) (see Section 2.3 for further details). The benchmark used for volatility estimation is the daily realized volatility provided by the Oxford-Man Institute's realized library (see, for example, Shephard & Sheppard, 2010). We find that, in general, our forecasting method significantly outperforms most of the MS-GARCH type models and all other quantile-based models. These results are robust in out-of-sample forecast comparisons with 500, 1000, 1500, and 2000 observations, respectively.

We further examine the forecasting performance of the QAR method over several subsamples. In this case, we partition the full sample for each index into three subsamples, ranging from March 2000 to December 2006 (pre-crisis), January 2007 to December 2009 (crisis), and January 2010 to February 2019 (post-crisis), respectively. We find that the results for the first and last subsamples are consistent with the full sample, which shows that, overall, the QAR forecasting method outperforms the MS-GARCH-type and other quantile-based models. Furthermore, we find that the QAR forecasting method statistically outperforms all models for all indices when the sample corresponding to the financial crisis is used. In addition, the results show that the performances of other quantile-based models also exceed those of the MS-GARCH- type models during this period. Lastly, we show that QAR models can explain the "volatility asymmetry" phenomenon.

This study contributes to the literature in four important ways. Firstly, we extend the work of Baur et al. (2012), which documents that the lower and upper quantiles of the returns' distribution exhibit dependences that occur in opposite directions from past returns. In addition to examining the direction of past returns' influence across various quantiles, our work also identifies the magnitude and persistence of such dependence patterns, which could be potentially useful in modelling returns' behaviour at the extremes of their distributions. Secondly, our study contributes to the literature by investigating stock market reactions and dependence structures based on market conditions. Our results are in concordance with several studies that have explored this issue. For instance, Sim and Zhou (2015) find that low oil price shock quantiles can affect US equities positively at high return quantiles. In a recent study, Trapin (2017) shows that autoregressive dependence is strong and persistent in both tails of the returns' distribution. We interpret our results in the following way. The lower quantiles, which contain negative returns, denote "bad times" for the market, while the upper quantiles, which contain positive returns, signal "good times" for the market. We find that future stock returns are negatively correlated with past returns when the market is experiencing 'good times', while they exhibit a positive autoregressive association during 'bad times'. These findings are similar to the findings of Veronesi (1999), which documents that stock markets overreact to bad news in good times and underreact to good news in bad times. Further, we notice a perceptible difference in the magnitude of the coefficients of significant lags at the

Table 1
Descriptive statistics.***

Index	Obs	Mean	Median	SD	Skewness	Kurtosis	JB	ADF
CAC 40	4843	−0.003	0.025	1.407	−0.089	8.005	5061***	−16.65***
DAX 30	4820	0.008	0.650	1.456	−0.075	8.715	6564***	−16.41***
FTSE 100	4791	0.003	0.031	1.144	−0.172	9.555	8602***	−17.63***
NIKKEI 225	4646	0.002	0.039	1.506	−0.428	9.276	7764***	−16.59***
S&P 500	4768	0.015	0.053	1.195	−0.197	11.234	13501***	−16.89***

This table reports summary statistics for five stock index returns, namely, the CAC 40, DAX 30, FTSE 100, NIKKEI 225, and S&P 500. The sample period is from 1 March 2000 to 28 February 2019, and daily observations are used. As the number of working days differs across markets, so does the number of observations across samples. The table shows the number of observations (Obs) as well as the mean, median, standard deviation (SD), skewness, and kurtosis for each stock index return series. We also report the test statistics and results for the Jarque-Bera (JB) test for normality and augmented Dickey-Fuller (ADF) test for stationarity.

*** Represents statistical significance at the 1% level.

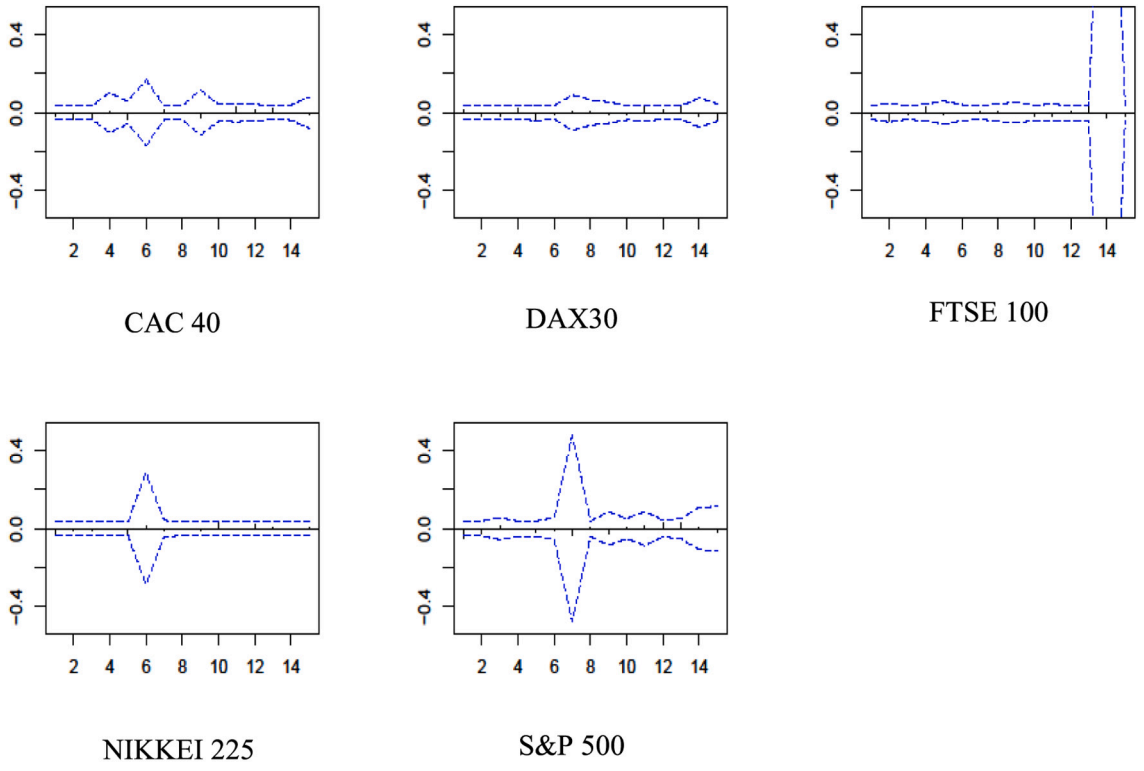

Fig. 1. QPACFs at the median.
This figure shows the sample quantile partial autocorrelation functions (QPACFs) of the five return series at $\tau = 0.5$. In each plot, the horizontal axis lists the lag orders, and the vertical axis lists the values of the sample QPACF, denoted by $\tilde{\varnothing}_{kk,\tau}$. The dashed lines correspond to 95% confidence bounds. The sample period is from March 2000 to March 2013.

two tails, with the magnitudes obtained for the right tail being larger than those obtained for the left tail. This observation corroborates the results of Žikeš and Baruník (2016), who find that the linear quantile regression models perform better at the right tail of the distribution for medium-horizon realized volatility forecasts.

Thirdly, we propose an alternative method for generating conditional volatility via the QAR model that accommodates the quantile dependence between stock returns. Our proposed method is built on the conditional autoregressive value-at risk-model of Taylor (2005), which, in turn, is based on the work of Engle and Manganelli (2004) and Pearson and Tukey (1965). In particular, Taylor's (2005) method generates variance forecasts based on linear functions of the square of the interval between symmetric quantiles. Unlike Taylor's method, which relies on Pearson and Tukey's work regarding forecasts, this paper applies the distribution constructed from the estimated quantiles directly to generate volatility forecasts. This feature imparts greater flexibility to our model in terms of incorporating temporal variations in the returns' distribution into volatility forecasts, resulting in better forecasting ability, even in turbulent market conditions. This attribute can be useful in asset pricing and risk management.

Finally, our method can also be applied to modelling "leverage effects" in asset returns. Several studies, such as Black (1976), Christie (1982), and Bekaert and Wu (2000), confirm that the conditional volatility of stock returns is asymmetric at both the market and the firm levels. In this study, we illustrate the link between the quantile autoregressive dependence structure obtained using the QAR model to this well-documented volatility feature of the return series. We confirm that the "leverage effect" of conditional volatility exists at the market level, as an increase in returns in the tails is associated with a decrease in returns' volatility, and vice versa. This result is consistent with the findings of Dimpfl and Baur (2016), who use inter-quantile ranges to explain asymmetric volatility.

The remainder of our paper is organized as follows. Sections 2 and 3 describe the methodology and data, respectively. Section 4 presents the empirical results, while Section 5 explores the volatility asymmetry using quantile autoregressive models. Section 6 concludes.

2. Methodology

2.1. Stock returns' quantile autocorrelation

The main purpose of this paper is to investigate stock returns' quantile autocorrelation and use the resulting autocorrelation pattern to generate volatility forecasts for financial assets. Li et al. (2015) define the quantile covariance for two random variables X and Y as follows:

$$qcov_\tau\{Y,X\} = E\{\psi_\tau(Y - Q_{\tau,Y})(X - E(X))\},$$

where $Q_{\tau,Y}$ is the τ^{th} unconditional quantile of Y, and the function $\psi_\tau(\omega) = \tau - I(\omega < 0)$ ($I(\cdot)$ being an indicator function). Correspondingly, the quantile correlation between two random variables is defined as:

$$qcor_\tau\{Y,X\} = \frac{qcov_\tau\{Y,X\}}{\sqrt{var\{\psi_\tau(Y - Q_{\tau,Y})\}var(X)}} = \frac{E\{\psi_\tau(Y - Q_{\tau,Y})(X - E(X))\}}{\sqrt{(\tau - \tau^2)\sigma_X^2}},$$

where $\sigma_X^2 = var(X)$.

Li et al. (2015) also introduce the quantile partial autocorrelation function (QPACF), which can be used to identify the autoregressive order of an observed time series in the context of quantile autoregressive

(QAR) model estimation. Specifically, the QPACF between y_t and y_{t-k} is defined as:

$$\varnothing_{kk,\tau} = qpcor_\tau\{y_t, y_{t-k}|\mathbf{z}_{t,k-1}\}$$

$$= \frac{E\left[\psi_\tau\left(y_t - \alpha_{2,\tau} - \beta'_{2,\tau}\mathbf{z}_{t,k-1}\right)y_{t-k}\right]}{\sqrt{(\tau-\tau^2)E\left(y_{t-k} - \alpha_1 - \beta'_1\mathbf{z}_{t,k-1}\right)^2}},$$

where k is a positive integer with $\mathbf{z}_{t,\,k-1} = (y_{t-1},\ldots,y_{t-k+1})'$, $(\alpha_1,\beta_1') = argmin_{\alpha,\,\beta}E(y_{t-k} - \alpha - \beta'\,\mathbf{z}_{t,\,k-1})^2$, and $(\alpha_{2,\,\tau},\beta_{2,\,\tau}') = argmin_{\alpha,\,\beta}E[\rho_\tau(y_t - \alpha - \beta'\mathbf{z}_{t,\,k-1})$. They show that for a given $\tau \in (0,1)$, $\sqrt{n}\tilde{\varnothing}_{kk,\tau} \rightarrow_d N(0,\Omega_3(\tau,\tau))$. Hence, for fixed τ, the significance of $\varnothing_{kk,\,\tau}$ can be determined via this asymptotic result.[1]

Following Li et al. (2015), we apply the sample QPACF to determine the dependence pattern between past returns and quantiles of the current returns' distribution, which then allows us to evaluate the predictive ability of past returns for different sections of the returns' distribution based on the varying order of significant lags.[2]

2.2. Volatility forecasting method

Our forecasting method comprises the following three steps. In step one, we specify the QAR model for stock returns using an appropriate lag structure. Let y_t be the stock returns at time t, then the QAR model is given by:

$$Q_\tau(y_t|y_{t-i}) = \beta_{0,\tau} + \beta_{1,\tau}y_{t-1} + \ldots + \beta_{i,\tau}y_{t-i}, \tag{2.1}$$

where $t = 1, \ldots T$, and $\tau = 0.01, \ldots, 0.99$. The optimum lag order i is determined via the method described in Section 2.1. We estimate 99 QAR models, i.e. one model at each quantile level. In step two, we obtain conditional density forecasts for stock returns, y_{T+m}, with $m = 1, \ldots, M$. Bondell, Reich, and Wang's (2010) method is used to estimate the conditional quantiles of y_t, thus avoiding the crossing-over problem associated with quantiles.[3] The details of this procedure are as follows:

(i) For $m = 1$, use the estimated QAR models to estimate the density forecast of y_{T+1} via the cubic smoothing spline method.
(ii) For $m = 2$, replace the variables y_{T+1} in the QAR models with the observed values at time $T + 1$, which are available at time $T + 2$.
(iii) Return to (i) with $m = 2$ to obtain the density forecast of y_{T+2} using the cubic smoothing spline method. By repeating the above steps, the density forecasts can be obtained for y_{T+m}, where $m = 1, \ldots, M$.

The final step is to obtain the volatility forecasts for y_{T+m} using the following procedure:

(i) Obtain a random sample of size N, which is 5000 in this study, from the density forecasts for the y_{T+m} obtained in step 2.
(ii) The conditional volatility forecasts of y_{T+m} are calculated as the sample standard deviations of the samples obtained in (i).

2.3. Benchmark volatility forecasting models

The following sections summarize the key features of the benchmark models whose volatility forecasting performances are subsequently compared with that of our proposed approach. In total, we use twelve benchmark models: six from the GARCH family, and six variants of the quantile approach. We begin with the latter set of models.

2.3.1. Quantile-based models

Pearson and Tukey (1965) use a simple interval approximation approach to estimating standard deviations, which then provides a foundation for further research on the use of quantile regression (QR) to predict volatility in stock markets. They show that standard deviations can be approximated by using the interval between symmetric quantiles, i.e. $Q(\theta)$ and $Q(1-\theta)$. More specifically, they use the following equation to estimate the standard deviation:

$$\widehat{\sigma} = \frac{\widehat{Q}(1-\theta) - \widehat{Q}(\theta)}{C(\theta)}, \tag{2.2}$$

where $\widehat{Q}(1-\theta)$ and $\widehat{Q}(\theta)$ are the estimated quantiles from a cumulative density function with probability θ, while $C(\theta)$ is a correction constant chosen to be 4.65, 3.92, and 3.25 for probabilities 0.01, 0.025, and 0.05, respectively.

Following Pearson and Tukey (1965), Taylor (2005) developed a new method for generating volatility forecasts via QR. This method involves two steps. First, the conditional autoregressive value-at-risk model (CAViaR) developed by Engle and Manganelli (2004) is used to produce value-at-risk (VaR) estimates at the required probability levels. Next, the conditional volatility is calculated based on the interval approximation method developed by Pearson and Tukey (1965). Pearson and Tukey's method estimates the standard deviations using the 98%, 95%, and 90% quantile intervals as:

$$\widehat{\sigma} = \frac{\widehat{Q}(0.99) - \widehat{Q}(0.01)}{4.65},$$

$$\widehat{\sigma} = \frac{\widehat{Q}(0.975) - \widehat{Q}(0.025)}{3.92},$$

$$\widehat{\sigma} = \frac{\widehat{Q}(0.95) - \widehat{Q}(0.05)}{3.25}.$$

Taylor (2005) uses a least squares (LS) regression of the squared errors, ε_t^2, which serve as proxies for the actual variance, on the square of the difference between symmetric quantile estimates, i.e. $\left(\widehat{Q}_t(1-\theta) - \widehat{Q}_t(\theta)\right)^2$, and adds that it is possible to estimate parameters for the approximations in the above equations in lieu of the fixed values, $C(\theta)$, in the denominators. The specification for such a least squares regression is:

$$\varepsilon_t^2 = \alpha + \beta\left(\widehat{Q}_t(1-\theta) - \widehat{Q}_t(\theta)\right)^2 + u_t, \tag{2.3}$$

where the coefficient β thus obtained is used to replace the denominator, $C(\theta)$,in eq. 2.2. Then, according to Taylor (2005), the one-step-ahead variance prediction is given by:

$$\sigma_{t+1}^2 = \widehat{\alpha} + \widehat{\beta}\left(\widehat{Q}_{t+1}(1-\theta) - \widehat{Q}_{t+1}(\theta)\right)^2,$$

where $\widehat{\alpha}$ and $\widehat{\beta}$ are the parameters estimated using Eq. 2.3.

Huang (2012) later extended the work of Taylor (2005) by proposing a new approach to generating volatility forecasts via QRs. Huang (2012) suggests that a single pair of quantiles, such as $\widehat{Q}_t(1-\theta)$ and $\widehat{Q}_t(\theta)$, might not explain the dynamic behaviours of volatility; thus, a series of uniformly spaced quantiles are used in his study to construct the LS regression. The uniformly spaced series of quantiles are expected to not only reflect the tail behaviours but also explain the entire distribution pattern. Huang (2012) proposes the following model:

[1] See Appendix 1 for further details.
[2] The process of obtaining the QPACF is detailed in Appendix 1.
[3] The R code for estimating the non-crossing quantile models are available in Professor Bondell's personal website (https://blogs.unimelb.edu.au/howard-bondell/#tab25).

$$\varepsilon_t^2 = \alpha + \beta F\left(\widehat{Q}_t(\theta)\right)^2, \tag{2.4}$$

where F(•) represents an unspecified function, and $\widehat{Q}_t\left(\frac{i}{100}\right)$ is the $\left(\frac{i}{100}\right)th$ conditional quantile of y_t for $i = 1, \ldots, m$. As shown in Huang (2012), there are three alternative functions F(•) with following specifications:

Standard deviation (SD): $F(\cdot) = \left(\frac{1}{m-1}\sum_{m=1}^{99}\left(Q(0.01m) - \overline{Q}\right)^2\right)^{\frac{1}{2}}$,

Weighted SD: $F(\cdot) = \left(\sum_{m=1}^{99} W\left(Q(0.01m) - \overline{Q}\right)^2\right)^{\frac{1}{2}}$,

Median SD: $F(\cdot) = \left(\frac{1}{m-2}\sum_{m=1}^{99}(Q(0.01m) - Q(0.5))^2\right)^{\frac{1}{2}}$,

where $\overline{Q}_t$ is the conditional mean of all fitted quantiles at time t, and W is set as $\left(\frac{i}{100}\right)\Big/25$ when $\frac{i}{100} \le 0.5$ and $\left(1-\frac{i}{100}\right)\Big/25$ otherwise. Hence, the volatility forecasts can be obtained from:

$$\sigma_{t+1}^2 = \widehat{\alpha} + \widehat{\beta} F\left(\widehat{Q}_{t+1}(\theta)\right)^2,$$

where $\widehat{\alpha}$ and $\widehat{\beta}$ are the parameters estimated in Eq. (2.4) and vary according to the choice of function F(.).

2.3.2. Markov-switching GARCH models (MSGARCH models)

The ARCH and GARCH models were introduced by Engle (1982) and Bollerslev (1986), respectively, and their variants are ubiquitous in volatility forecasting research as well as in practice. Over the past three decades, financial literature has indicated that the GARCH(1,1) and GJR-GARCH(1,1) models tend to deliver more accurate forecasts than other GARCH-type models relying on higher-order lags. One inherent disadvantage of the GARCH-type models is that they do not incorporate changes in means. One way to overcome this shortcoming is to use MS-GARCH models, as they allow the parameters of the GARCH models to vary over time according to a latent discrete Markov Process (Ardia et al., 2019).[4] This feature, to some extent, is consistent with our forecasting method, which allows the parameters of the QAR models to vary over time in terms of both persistence and magnitude. MS-GARCH models are indeed a difficult benchmark to beat in volatility forecasting applications; hence, we compare the forecasts produced using our method with those of the MS-GARCH models.

We follow Haas, Mittnik, and Paolella (2004) when estimating the MS-GARCH models. According to Ardia et al. (2019), the general MS-GARCH specification can be expressed as:

$$\left(y_t | (s_t = k, I_{t-1}) \sim D\left(0, h_{k,t}, \xi_k\right)\right),$$

where I_{t-1} is the information set observed up to time $t-1$, and s_t, defined on the discrete space $\{1, \ldots, K\}$, characterizes the MS-GARCH model.[5] The variance in this model is filtered using a measurable function $h(.)$, conditional on regime $s_t = k$, such that:

$$h_{k,t} \equiv h\left(y_{t-1}, h_{k,t-1}, \boldsymbol{\theta}_k\right),$$

where $h(\cdot)$ not only defines the filter for the conditional variance but also ensures its positiveness given the information set I_{t-1}.

The MS-GARCH(1,1) model is given by the following expression:

$$h_{k,t} = \alpha_{0,k} + \alpha_{1,k} y_{t-1}^2 + \beta_k h_{k,t-1}$$

for $k = 1, \ldots, K$. Here, $\alpha_{0,k}$, $\alpha_{1,k}$, and β_k are parameters in the regime k. In this case, $\boldsymbol{\theta}_k = (\alpha_{0,k}, \alpha_{1,k}, \beta_k)^T$represents the vector of the model parameters. The MS-GJRGARCH(1,1) model, on the other hand, is given by:

$$h_{k,t} = \alpha_{0,k} + \left(\alpha_{1,k} + \alpha_{2,k} I\{y_{t-1} < 0\}\right) y_{t-1}^2 + \beta_k h_{k,t-1},$$

where $I\{\cdot\}$ is an indicator function with value one if the condition holds and zero otherwise. In this case, we have $\boldsymbol{\theta}_k = (\alpha_{0,k}, \alpha_{1,k}, \alpha_{2,k}, \beta_k)^T$. Typically, the parameter $\alpha_{2,k}$ reflects the presence of the leverage effect in the conditional volatility for regime k.

3. Data

We examine the stock return quantile autocorrelation for five stock indices, namely, the CAC 40, DAX 30, FTSE 100, NIKKEI 225, and S&P 500. The return series is calculated as the logarithmic difference of the closing index prices from time $t-1$ to time t, so $R_t = ln\,(p_t/p_{t-1}) * 100$. Stock index data are from the Datastream market information service provided by Thomson Reuters. We use daily data for a sample period from 1 March 2000 to 28 February 2019. The sample sizes for indexes differ slightly from each other because of different numbers of trading days in each stock market.

Table 1 presents the descriptive statistics. Along with the usual summary statistics, including the mean, median, standard deviation (SD), skewness, and kurtosis for each index return, we also report the test statistics and results for the Jarque-Bera (JB) test for normality and augmented Dickey-Fuller (ADF) test for stationarity. As shown in Table 1, the average daily return of these return series is close to zero. The negative skewness and high kurtosis values indicate that all the financial markets considered in this study experienced a high downside risk and unexpected extreme returns. In addition, the results of the Jarque-Bera test show that these return series do not follow the normal distribution. The results from the augmented Dickey-Fuller test show that the null hypothesis of a unit root is rejected at the 1% level of significance in all cases. Thus, all return series exhibit trend stationarity.

4. Empirical results

4.1. Quantile dependence pattern of stock returns

This section reports the results of the QPACF analyses of the stock returns for the five stock indices considered. As described in Section 2.1, we apply the sample QPACF to examine the impact of past returns on current returns at different quantile levels in order to determine the optimal lag order at each quantile level. We use a relatively full set of quantile levels ranging from 0.1 to 0.9, increasing in steps of 0.05, to characterize the quantile dependence pattern of the stock returns over the entire distribution.

Figs. 1 to 6 report the QPACFs of the five return series at various quantile levels. Specifically, Fig. 1 reports the QPACFs of the five return series at the median level, i.e. 50th percentile, and Figs. 2 to 6 show the QPACFs of the return series at quantile levels ranging from 0.1 to 0.9, bar the median. In each plot, the horizontal axis depicts the order of the lags, and the vertical axis depicts the estimated QPACF (denoted by $\tilde{\varnothing}_{kk,\tau}$). The dashed lines correspond to 95% confidence bounds. Following Li et al. (2015), we test for quantile autocorrelation for up to

[4] The conditional volatility estimated in GARCH-type models is driven by shocks in the observed time series, while, in stochastic volatility models, conditional volatility is driven by volatility-specific shocks (see Kastner, 2016). Compared to the former method, estimation of stochastic forecasting models has proved to be difficult; as a result, they are not as widely used as GARCH models (Taylor, 2005).

[5] Although the parametric formulation of the conditional distribution $D(0, h_{k,t}, \xi_k)$ can be different across regimes, we use the same conditional distribution across each regime in this study for simplicity. The conditional distributions considered in this study are the normal distribution, Student's t distribution, and skewed Student's t distribution.

15 lags. This analysis determines the optimal lag order to use for each return series at any given quantile.

From Fig. 1, we deduce that the autoregressive dependence in stock returns is weak in the case of the return series for the CAC 40, DAX 30, FTSE 100, and NIKKEI 225, as none of the lags are significant.[6] For the S&P 500, we find that a mild autocorrelation between stock returns at lag 1 is significant at the median. This finding is consistent with the weak form of the efficient market hypothesis (EMH) proposed by Fama (1970). Our finding suggests that when the financial market is stable, past returns have no predictive power for future returns. However, the situation is different when we focus on other quantile levels, as discussed below.

For example, consider the dependence pattern obtained for the CAC 40 at various quantiles of the returns' distribution. Fig. 2 reveals that for the quantile level $\tau = 0.1$, lags 1 and 4 are significant at a 95% confidence level. In contrast, the first two lags are significant at, or are very close to, the 95% confidence bounds for the quantile levels from the 15th to 30th percentile. This autoregressive dependence wanes as we move towards the central quantiles. At the 55th and 60th percentiles, we find that the first three lags and the fifth lag are statistically significant. Moreover, the number of significant lags increases as we consider the 65th and higher percentiles. Another interesting result is that at the lower end of the quantiles, the signs of the lag coefficients are positive. We interpret this finding as the likelihood that a negative return in the left tail is followed by another negative return, i.e. the current stock return occurs in the same direction as past returns. In contrast to the lower quantiles, the signs of the lag coefficients are negative in the upper quantiles, which means that in the right tail, a relatively large return will be followed by a smaller return.

Table 2 summarizes the significant number of lags for each return series for different quantiles. This table shows that the quantile dependence pattern for CAC 40 holds generally for the other four stock indices, although the identified order of significant lags can differ at specific quantile levels. To summarize, we find that the lower quantiles of the current returns' distribution depend positively on past returns, while the upper quantiles exhibit a negative dependence on past returns. These findings suggest that a high-magnitude negative return is likely to be followed by a negative return of lower magnitude when the left tail of the distribution is being considered, and a positive return of a high magnitude is likely to be followed by a return of lesser magnitude when considering the right tail of the distribution. These results also suggest that when the financial markets are in extreme conditions, such as during the financial crisis of 2008–9, stock returns exhibit a more pronounced dependence pattern, both in terms of the magnitudes of the coefficients and the number of significant lags. Our findings are consistent with Baur et al. (2012), which documents that the lower and upper quantiles exhibit different dependence behaviours on past returns and that such a pattern holds even when accounting for several stock-specific characteristics, such as market capitalization or market risk exposure. In the context of this study, we observe a similar pattern for market index returns. In contrast with Baur et al. (2012), we not only investigate the direction of the influence of past returns across various quantiles of the current returns' distribution but also identify the degrees of persistence of such dependence patterns by identifying the number of significant lags at various points in the returns' distribution.

4.2. QAR specification

As reported in the preceding section, the direction and persistence of the influence of past returns varies from one section of the returns' distribution to another. To incorporate this finding in our analysis, we divide the full quantile interval (0, 1) into 6 subintervals with unequal spans. These subintervals are constructed by combining the quantiles exhibiting similar dependence patterns. The six quantile ranges are (0.1, 0.15), (0.16, 0.25), (0.26, 0.55), (0.56, 0.75), (0.76, 0.84), and (0.85, 0.99), respectively. This exercise reduces the number of regressions required for fully specifying the QAR model and evaluating its forecasting performance greatly. Specifically, six QAR specifications corresponding to the six subintervals are specified for each stock index. For each interval, we incorporate different numbers of lags into the QAR specification to reflect the variation in the predictive ability of past returns across the corresponding quantiles of the returns' distribution.[7]

Table 3 summarizes the number of lags used for the corresponding quantile ranges. The estimation results are similar across all indexes. For illustration, the estimation results for the S&P 500 sample are shown in Appendix 3. As can be seen from each table, the estimated coefficients for the intercept increase with quantile level, which implies that the stock returns are larger for the upper quantiles and lower for the lower quantiles. With respect to the other autoregressive coefficients, we find that the estimated coefficients are close to zero for returns around the median of the returns' distribution, which implies that yesterday's return is irrelevant to today's return around the central part of the returns' distribution. Similar to the QPACF analysis presented in Section 4.1, the estimated autoregressive parameter(s) becomes statistically significant as we move away from the middle towards the tails of the returns' distribution, but the association is positive in the left tail and negative in the right tail. Our finding is consistent with Baur et al. (2012), which reports a decreasing pattern in the autoregressive coefficient estimates, especially for AR(1) terms, moving from the left tail to the right tail of the returns' distribution. Having specified our QAR model for various quantile ranges, we will now present the forecasting performance of this method.

4.3. Forecasting evaluation

Our forecasting methodology involves dividing the full sample into two sets - training and testing datasets. The training dataset is used for parameter estimation, and the testing dataset is used for forecasting evaluation. Table 4 presents information on the full sample and the subsamples chosen for evaluating the volatility forecasting performance. Specifically, we adopt two alternative ways to examine the forecasting results. The first option involves dividing the full sample into two parts and examining the forecasting performance with the testing dataset. Another option is to divide the full sample into subsamples based on the state of the economy (see Method 2 below), then split each of the subsamples into two sets for evaluation. In each case, the size of the testing dataset is presented in parentheses. Some of the estimation results for the first method are shown in Section 4.2. For the second option, we respecify all the forecasting models to accommodate the distribution specific to each subsample.

In each case, our forecasting results are compared with other widely used volatility forecasting methods to evaluate the out-of-sample predictive performance of each forecasting model. The forecast efficiency of all the models is measured relative to the daily non-parametric measure of the stock index volatility provided by the Oxford-Man Institute's realized library (also see Shephard & Sheppard, 2010). This proxy of the so-called "true volatility" for a given day depends solely on the high-frequency financial data collected that day. To evaluate the efficacy of the volatility forecasts produced by different models, we use the mean squared error (MSE) criterion and the Diebold and Mariano (1995) test

[6] It seems that lags 2 and 3 for CAC 40, lag 2 for FTSE 100, and lag 1 for NIKKEI 225 are very close to the confidence bounds, although they are insignificant at the 5% significance level.

[7] Selection of the appropriate lag order is based on Table 2 and Figs. 2 to 6.

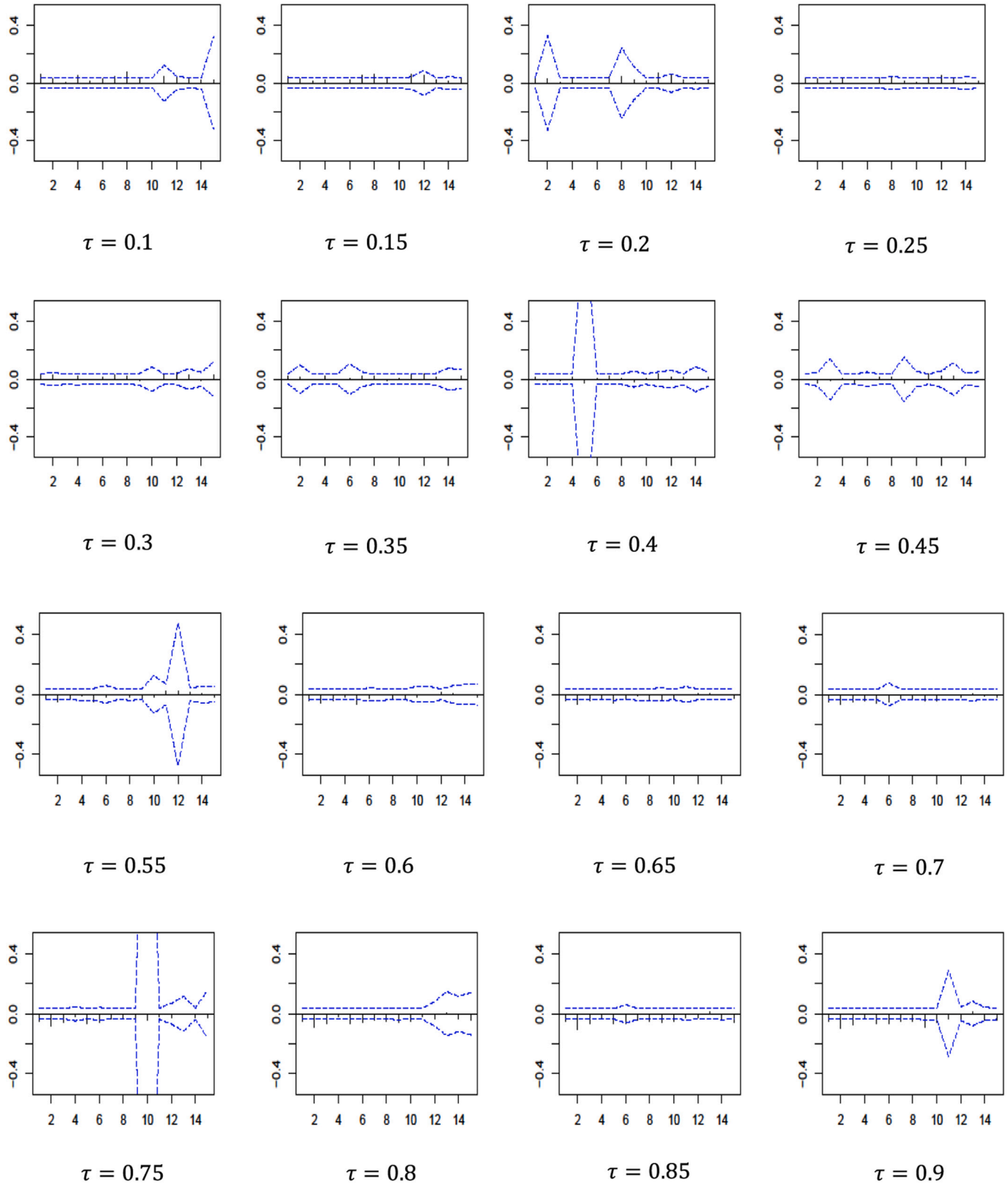

Fig. 2. QPACFs for the CAC 40 at various quantile levels.
This figure shows the sample quantile partial autocorrelation function (QPACF) values for the CAC 40 return series at τ = 0.1, 0.15, 0.2, 0.25, 0.3, 0.35, 0.4, 0.45,0.55, 0.6, 0.65, 0.7, 0.75, 0.8, 0.85, and 0.9. In each plot, the horizontal axis lists the lag orders, and the vertical axis lists the values of the sample QPACF, denoted by $\tilde{\varnothing}_{kk,\tau}$. The dashed lines correspond to 95% confidence bounds. The sample period is from March 2000 to March 2013.

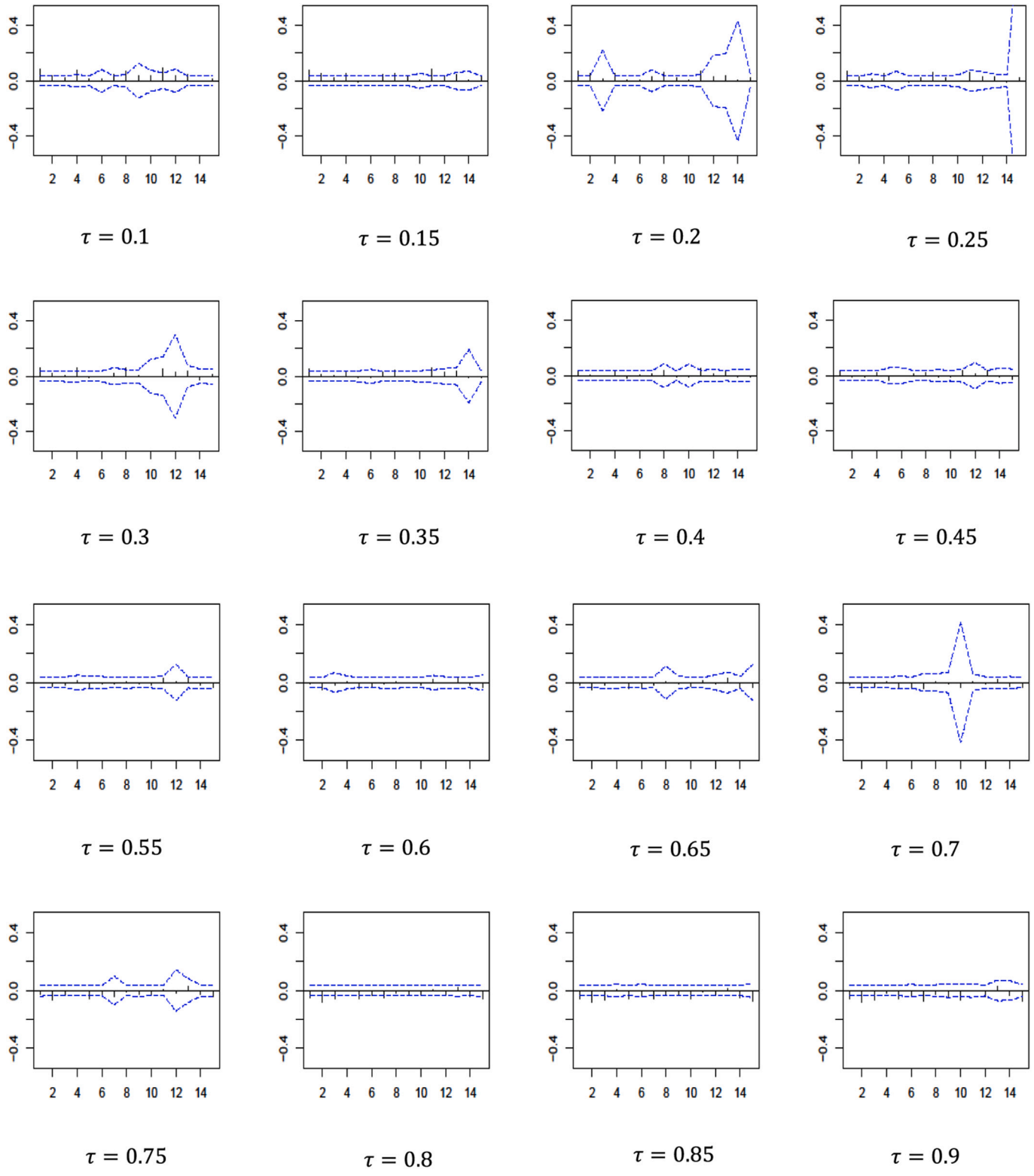

Fig. 3. QPACFs for the DAX 30 at various quantile levels.
This figure shows the sample quantile partial autocorrelation function (QPACF) values for the DAX 30 return series at τ = 0.1, 0.15, 0.2, 0.25, 0.3, 0.35, 0.4, 0.45,0.55, 0.6, 0.65, 0.7, 0.75, 0.8, 0.85, and 0.9. In each plot, the horizontal axis lists the lag orders, and the vertical axis lists the values of the sample QPACF, denoted by $\tilde{\varnothing}_{kk,\tau}$. The dashed lines correspond to 95% confidence bounds. The sample period is from March 2000 to March 2013.

(hereafter, the DM test).[8]

The MSEs of the volatility forecasts based on 1500 out-of-sample predictions are reported in Table 5. The left column lists all the forecasting models considered in this study, in particular, the QAR model, the six variants of the GARCH-type models, and the six quantile-based models. The GARCH-type models include the MS-GARCH(1,1) model and the MS-GJRGARCH(1,1) model, with each then combined with the assumption that the stock index returns follow a normal distribution (N), Student's t distribution (ST), and skewed Student's t distribution (SST), respectively. In each case, we consider two regimes, i.e. $k = 2$. The quantile-based models contain the three forecasting models proposed by Taylor (2005), termed Taylor 98, Taylor 95, and Taylor 90, along with the three variants of the forecasting model proposed by Huang (2012), labelled Huang SD, Huang WSD, and Huang MSD.

As reported in Table 5, we find that the QAR method has a lower MSE than most MS-GARCH models and other quantile-based models. In particular, our forecasting method delivers the best forecasting performance for the NIKKEI 225 stock index, as the QAR method has the lowest MSE in all cases. The results of the DM test show that the improvement in forecasting is statistically significant at the 1% level. For the other stock indices, our forecasting method outperforms the MS-GARCH-type models and all other quantile-based models. For example, compared with the MS-GARCH(1,1) model with the ST and MS-GJRGARCH(1,1) model with the SST, our method generates a lower MSE and improves the forecasting performance significantly. However, the results show that the MS-GJRGARCH(1,1) with the N performs marginally better.

In Appendix 2, we show the prediction results for all models when considering other out-of-sample periods with 500, 1000, and 2000 observations, respectively. The results show that the QAR forecasts outperform most of the MS-GARCH-type models and that the reduction in MSE is significant at the 1% level of significance. For example, our method delivers a better forecasting performance than all the MS-GARCH(1,1) models, except for the MS-GARCH(1,1) with the SST, when taking 2000 out-of-sample observations into consideration. In addition, the QAR method outperforms all the other quantile-based models for all the stock indices over every testing period. These results further support the robustness of the outperformance of the QAR method.

Next, we discuss the forecasting results obtained when our full sample is split into three subsample periods. Table 6 presents the forecasting results of all models for the three subsamples, namely pre-crisis (Panel A), crisis (Panel B), and post-crisis (Panel C). As shown in Panel A, the QAR forecasts have a smaller MSE than the MS-GARCH(1,1) model combined with any distribution for the CAC 40, DAX 30, and NIKKEI 225 indexes. For the S&P 500, the QAR forecasts outperform the MS-GARCH(1,1) forecasts obtained via both the ST and SST. The DM test confirms that the difference in performance is statistically significant at the 1% significance level. However, the MS-GJRGARCH(1,1) model generates a lower MSE than the QAR model, and the reduction in MSE is significant at the 1% level. The results for the NIKKEI 225 are encouraging because they show that our forecasting method outperforms all the other models considered in this study. The DM test again confirms that the improvement is significant at the 1% level.

Panel B presents the forecasting results for all models for the financial crisis period spanning January 2007 to December 2009. During this period, the QAR model outperforms all other models statistically for all the indices analysed. Moreover, all the quantile-based models have better forecasting performances than the MS-GARCH-type models for this turbulent period according to all the evaluation measures used in the study. The DM test confirms that the forecasting improvements made by quantile-based models are statistically significant at all the usual significance levels. This finding suggests that during periods when extreme stock returns are observed frequently, using a quantile-based model is more appropriate than using a model with a pre-determined distribution.

Panel C of Table 6 reports the forecasting results of all models for the post-crisis period from January 2010 to February 2019. Overall, the results show that the QAR forecasting method outperforms all models in generating the conditional volatility forecasts for the NIKKEI 225 return series, and the DM test statistic is significant at the 1% level. Additionally, for the CAC 40, our forecasting method delivers the lowest MSE of all, and the DM test confirms that the difference is significant at the 1% level, except in the case of the MS-GARCH(1,1) with the N. Consistent with previous findings, the MS-GJRGARCH(1,1) with the N performs well in the prediction of the conditional volatility for the DAX 30, FTSE 100, and S&P 500. On the other hand, the MS-GJRGARCH(1,1) with the ST and SST significantly underperform relative to the QAR model for these three indices, indicating that the forecasting performance of parametric distribution-based models is susceptible to pre-determined distribution assumptions. Although some MSE values for MS models are smaller than those for the QAR models, the two models have equal predictive abilities. Considering the performance of all models across all three subsamples suggests that the QAR model outperforms the MS-GARCH and all other quantile-based models.

The above results confirm the predictive power of quantile-based models used in volatility forecasting compared with traditional models, like GARCH-type models, and our results are similar to Taylor (2005) and Huang (2012). However, compared with the results in Taylor (2005) and Huang (2012), our model obtains relatively better results within quantile-based models. To the best of our knowledge, Taylor (2005) was the first study to propose a quantile regression method to generate variance forecasts, which is based on the CAViaR model of Engle and Manganelli (2004) and the simple approximation method of Pearson and Tukey (1965). In Taylor's work, the variance forecasts were generated on the basis of linear functions of the square of the interval between symmetric quantiles. The method proposed in this paper differs from Taylor's procedure of relying on the approximation method proposed in Pearson and Tukey (1965), and directly applies the distribution constructed from the estimated quantiles to generate variance forecasts.

5. Volatility asymmetry

The leverage effect refers to the observed negative correlation between an asset's returns and the changes in its volatility (see, for example, Nelson, 1991; Engle & Ng, 1993; and Aït-Sahalia, Fan, Laeven, Wang, & Yang, 2017). Previous literature in this area considers three distinct economic channels to explain this relationship: the 'leverage effect' in Black (1976), the 'volatility feedback effect' in Campbell and Hentschel (1992) and Bekaert and Wu (2000), and the 'self-exciting behaviour' theory in Azizpour, Giesecke, and Schwenkler (2018). Unlike the studies that consider economic channels, this paper explains the interaction between asset returns and their volatility using a quantile regression (QR) method.[9] We provide a new perspective to interpret the relationship between asset returns and volatility.

Figs. 2 to 6 and in-sample estimation (see Appendix 3) suggest that there is a decreasing pattern in the autoregressive coefficient estimates, especially for the AR (1) term, moving from the lower to upper quantiles. As reported in Section 4.1, past returns affect future returns positively in

[8] The DM test is a popular comparison method for non-nested forecasting models, which is widely used by many recent related papers (e.g. Zhang, Lei, & Wei, 2020; Zhang, Ma, & Wei, 2019, Choi & Shin, 2019, and Gong & Lin, 2018). Here, we use DM test to examine whether the QAR Model outperforms the GARCH-type models.

[9] Carr and Wu (2017) examined these three economic channels on the index option pricing, and they found that the contribution of these three channels are different in companies with different business types and capital structure behaviours.

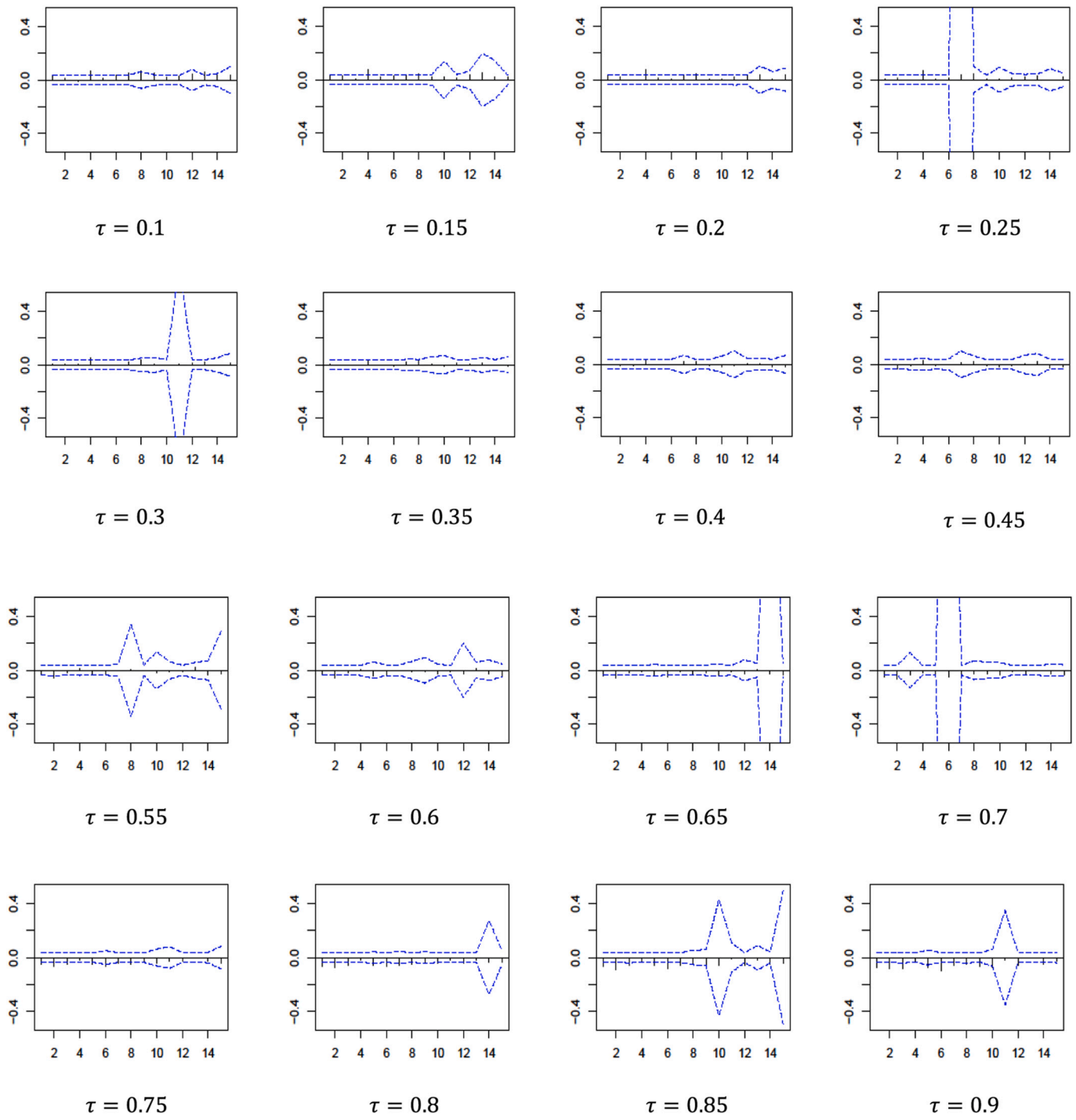

Fig. 4. QPACFs for the FTSE 100 at various quantile levels.
This figure shows the sample quantile partial autocorrelation function (QPACF) values for the FTSE 100 return series at $\tau = 0.1, 0.15, 0.2, 0.25, 0.3, 0.35, 0.4, 0.45, 0.55, 0.6, 0.65, 0.7, 0.75, 0.8, 0.85$, and 0.9. In each plot, the horizontal axis lists the lag orders, and the vertical axis lists the values of the sample QPACF, denoted by $\tilde{\mathcal{O}}_{kk,\tau}$. The dashed lines correspond to 95% confidence bounds. The sample period is from March 2000 to March 2013.

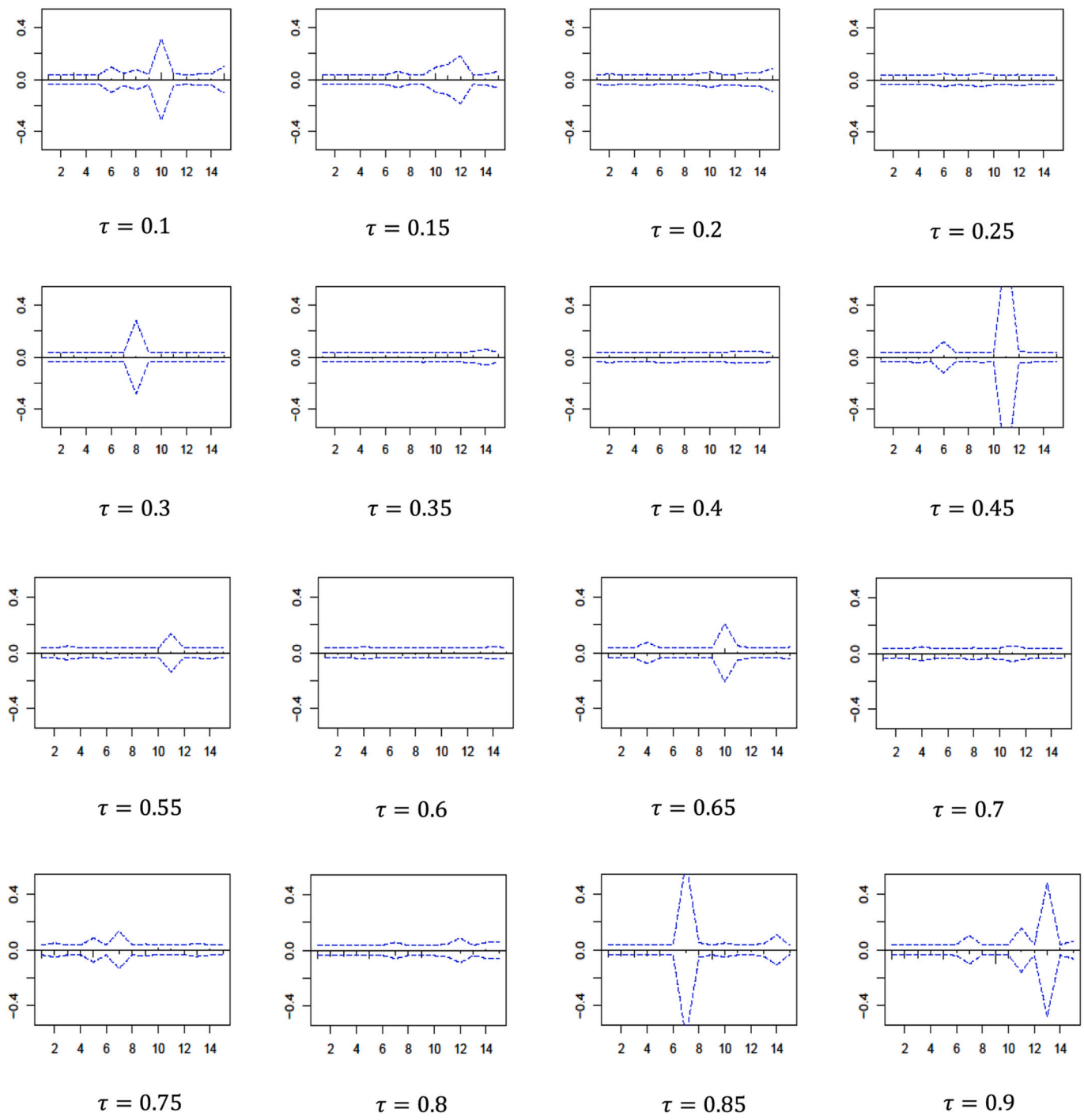

Fig. 5. QPACFs for the Nikkei 225 at various quantile levels.
This figure shows the sample quantile partial autocorrelation function (QPACF) values for of the NIKKEI 225 return series at $\tau = 0.1, 0.15, 0.2, 0.25, 0.3, 0.35, 0.4, 0.45, 0.55, 0.6, 0.65, 0.7, 0.75, 0.8, 0.85$, and 0.9. In each plot, the horizontal axis lists the lag orders, and the vertical axis lists the values of the sample QPACF, denoted by $\tilde{\varnothing}_{kk,\tau}$. The dashed lines correspond to 95% confidence bounds. The sample period is from March 2000 to March 2013.

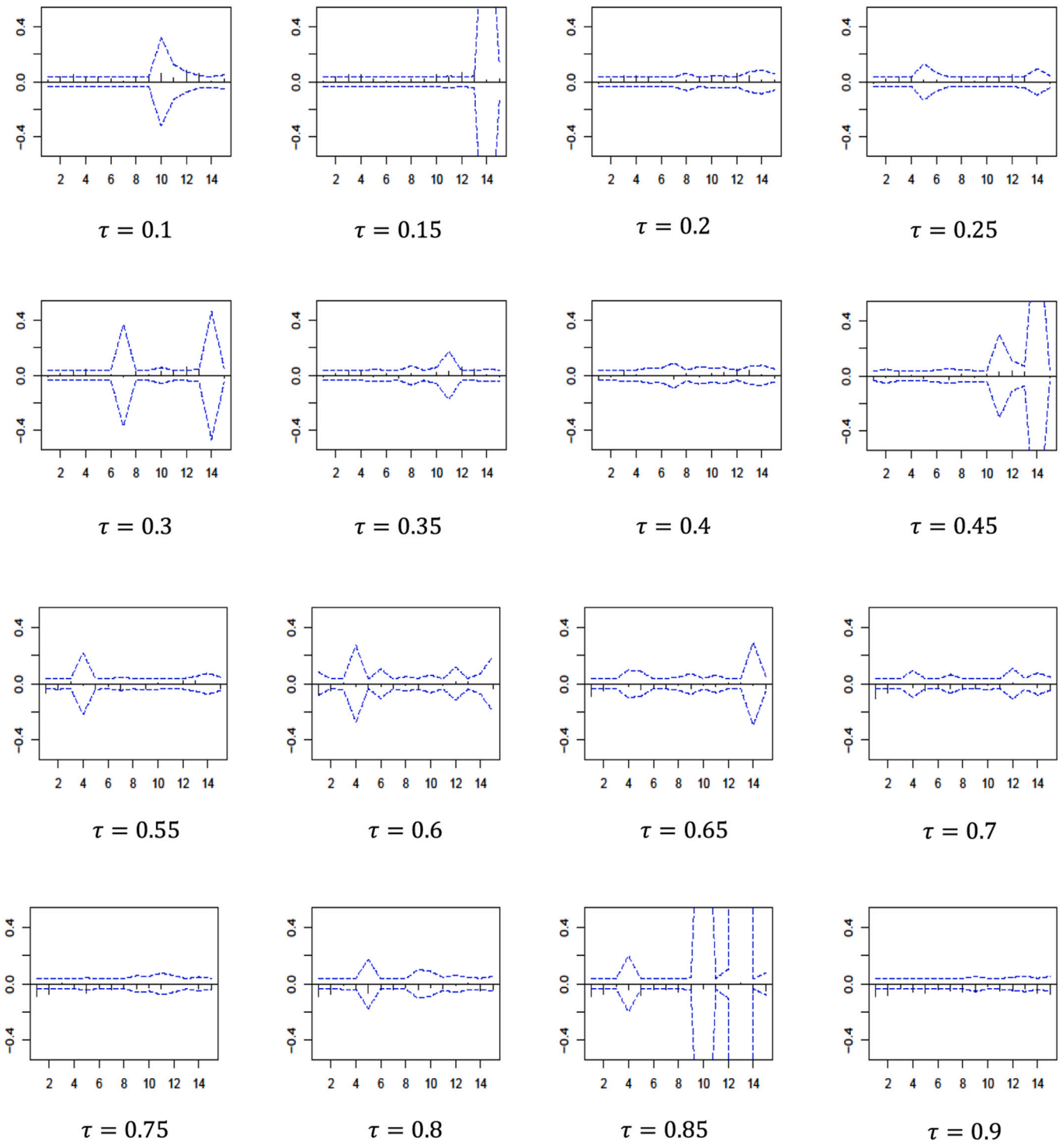

Fig. 6. QPACFs for the S&P 500 at various quantile levels.
This figure shows the sample quantile partial autocorrelation function (QPACF) values for the S&P500 return series at $\tau = 0.1, 0.15, 0.2, 0.25, 0.3, 0.35, 0.4, 0.45, 0.55, 0.6, 0.65, 0.7, 0.75, 0.8, 0.85$, and 0.9. In each plot, the horizontal axis lists the lag orders, and the vertical axis lists the values of the sample QPACF, denoted by $\tilde{\varnothing}_{kk,\tau}$. The dashed lines correspond to 95% confidence bounds. The sample period is from March 2000 to March 2013.

Table 2
Summary of the significant lags for QPACFs at different quantiles.

τ	0.1	0.15.	0.2	0.25	0.3	0.35	0.4	0.45
CAC 40	**1,4**	**1**	*	*	*	*	*	*
	(+)	(+)	(+)	(+)	(+)	(+)	(++)	(++)
DAX 30	**1,4**	**1,2,4**	**1,2,4**	**1,4**	**1,4**	**1**	*	*
	(+)	(+)	(+)	(+)	(+)	(++)	(++)	(++)
FTSE 100	**4**	**4**	**4**	**4**	**4**	*	*	*
	(+)	(+)	(+)	(+)	(+)	(++)	(++)	(++)
NIKKEI 225	*	*	**3**	*	*	*	*	*
	(+)	(+)	(+)	(+)	(+)	(++)	(++)	(++)
S&P 500	**3**	**3,4**	**3,4**	*	**4**	*	*	**1**
	(+)	(+)	(+)	(+)	(++)	(++)	(++)	(++)
τ	0.55	0.6	0.65	0.7	0.75	0.8	0.85	0.9
CAC 40	**2**	**1,2,3,5**	**1,2,3,5**	**1,2,3,4,5**	**1,2,3,5,6**	**1,2,3,5…**	**1,2,3,5…**	**1,2,3,5…**
	(−)	(−)	(−)	(−)	(−)	(−)	(−)	(−)
DAX 30	*	**2**	**2**	**2**	**2,5**	**2,3,5,7**	**1,2,3,5,7**	**1,2,3,5,7**
	(++)	(++)	(++)	(++)	(−)	(−)	(−)	(−)
FTSE 100	**2**	**2**	**1,2**	**1,2**	**1,2,3,5…**	**1,2,3,5…**	**1,2,3,5…**	**1,2,3,5…**
	(++)	(++)	(−)	(−)	(−)	(−)	(−)	(−)
NIKKEI 225	*	*	*	**1**	**1**	**1,2,3,5**	**1,2,3,4,5**	**1,2,3,5**
	(++)	(−)	(−)	(−)	(−)	(−)	(−)	(−)
S&P 500	**1**	**1,2**	**1,2**	**1,2**	**1,2**	**1,2**	**1,2,5,…,9**	**1,2,4,…,9**
	(++)	(++)	(−)	(−)	(−)	(−)	(−)	(−)

This table summarizes the identified significant lags of the QPACFs for the five stock return series at different quantiles ranging from 0.1 to 0.9 in steps of 0.05. In each row, numbers in bold script are used to indicate the significant lags, and asterisks indicate the absence of significant lags in the corresponding quantile ranges. The symbols "+", "-", and "++" presented in parentheses represent the positive, negative, and mixed impact past returns have on the current returns at the corresponding quantile levels.

the left tail and negatively in the right tail. This finding, in fact, confirms a well-known empirical phenomenon, i.e. the "leverage effect" in finance, which states that asset volatility is negatively related to its returns. Next, we explain how our model can explain this leverage effect.

Fig. 7 shows the "leverage effects" of conditional volatility via the QAR model. In each plot, for illustration purposes, we use two curves (blue and red) to represent the distribution of the stock returns of a financial market, where the blue density curve has a greater variance than the red one, and both curves have area τ. Consider two scenarios with respect to the future direction of the stock returns. On one side, there is an increase in stock returns, and, on the other side, there is a decrease in stock returns.

Referring to our basic model presented in Table 3 with the following general specification:

$$Q(y_t|F_{t-1}) = \beta_{0,\tau} + \beta_{1,\tau}y_{t-1} + \ldots + \beta_{i,\tau}y_{t-i}$$

and based on the results presented in Table 2, we infer that in the left tail, the coefficients $\beta_{1,\ \tau}\ldots\beta_{i,\ \tau}$ have a positive effect on the fitted conditional quantiles; however, the effect is negative in the right tail. Thus, in plot (a) of Fig. 7, when there is an increase in stock returns in the future, i.e. $y_{t-1}^{(1)} < y_{t-1}^{(2)}$, there will be a corresponding increase in the fitted quantiles, i.e. $Q_{y_{t,\ \tau}}{}^{(1)} < Q_{y_{t,\ \tau}}{}^{(2)}$. While, in the right tail, whenever there is an increase in stock returns in the future, i.e. $y_{t-1}^{(1)} < y_{t-1}^{(2)}$, there will be a decrease in the fitted quantiles, i.e. $Q_{y_{t,\ \tau}}{}^{(1)} > Q_{y_{t,\ \tau}}{}^{(2)}$. Therefore, the distribution of stock returns contracts.

To the contrary, in plot (b), when there is a decrease in future stock returns, i.e. $y_{t-1}^{(1)} > y_{t-1}^{(2)}$, there will be a corresponding decrease in the fitted quantiles in the left tail, i.e., $Q_{y_{t,\ \tau}}{}^{(1)} > Q_{y_{t,\ \tau}}{}^{(2)}$, as, in this part, the autoregressive coefficients have a positive effect on the fitted

Table 3
The specifications of QAR models for different quantile ranges.

Lag	Model	τ
5	$Q_\tau(y_t\|F_{t-1}) = \varnothing_0(\tau) + \varnothing_1(\tau)y_{t-1} + \ldots + \varnothing_5(\tau)\,y_{t-5}$	(0.01, 0.15)
4	$Q_\tau(y_t\|F_{t-1}) = \varnothing_0(\tau) + \varnothing_1(\tau)y_{t-1} + \ldots + \varnothing_4(\tau)\,y_{t-4}$	(0.16, 0.25)
1	$Q_\tau(y_t\|F_{t-1}) = \varnothing_0(\tau) + \varnothing_1(\tau)y_{t-1}$	(0.26, 0.55)
2	$Q_\tau(y_t\|F_{t-1}) = \varnothing_0(\tau) + \varnothing_1(\tau)y_{t-1} + \varnothing_2(\tau)\,y_{t-2}$	(0.55, 0.75)
5	$Q_\tau(y_t\|F_{t-1}) = \varnothing_0(\tau) + \varnothing_1(\tau)y_{t-1} + \ldots + \varnothing_4(\tau)\,y_{t-4} + \varnothing_5(\tau)\,y_{t-5}$	(0.76, 0.84)
9	$Q_\tau(y_t\|F_{t-1}) = \varnothing_0(\tau) + \varnothing_1(\tau)y_{t-1} + \varnothing_2(\tau)\,y_{t-2} + \ldots + \varnothing_9(\tau)\,y_{t-9}$	(0.85, 0.99)

This table shows the specifications of QAR models for different quantile ranges for all five return series. The first column reports the number of lags used in the QAR specifications for the quantile ranges $\tau \in (0.01, 0.15)$, $\tau \in (0.16, 0.25)$, $\tau \in (0.26, 0.55)$, $\tau \in (0.76, 0.84)$, and $\tau \in (0.85, 0.99)$, respectively. In each model, F_{t-1} represents the information set available up to time *t-1*.

Table 4
Full sample and subsample periods used for forecasting performance evaluation.

	Method 1	Method 2		
Market Index	Full sample	Subsample period: pre-crisis	Subsample period: crisis	Sub-sample period: post-crisis
CAC 40	Mar. 2000 – Feb.2019 (1500)	Mar. 2000 – Dec. 2006 (500)	Jan. 2007 – Dec. 2009 (300)	Jan. 2010 – Feb. 2019 (500)
DAX 30	Mar. 2000 – Feb.2019 (1500)	Mar. 2000 – Dec. 2006 (500)	Jan. 2007 – Dec. 2009 (300)	Jan. 2010 – Feb. 2019 (500)
FTSE 100	Mar. 2000 – Feb.2019 (1500)	Mar. 2000 – Dec. 2006 (500)	Jan. 2007 – Dec. 2009 (300)	Jan. 2010 – Feb. 2019 (500)
NIKKEI 225	Mar. 2000 – Feb.2019 (1500)	Mar. 2000 – Dec. 2006 (500)	Jan. 2007 – Dec. 2009 (300)	Jan. 2010 – Feb. 2019 (500)
S&P 500	Mar. 2000 – Feb.2019 (1500)	Mar. 2000 – Dec. 2006 (500)	Jan. 2007 – Dec. 2009 (300)	Jan. 2010 – Feb. 2019 (500)

This table presents information on the full sample and subsample periods chosen for evaluating the volatility forecasting performance. The first column lists the five stock market indices considered in this study, and the remaining columns lists the information on the full samples and subsample periods. Each sample is divided into two sets, i.e. training and testing datasets. The training dataset is used for model estimation, and the testing dataset is used for forecasting performance evaluation. Then each full sample is divided into three parts (see Method 2), and each subsample is split into training and testing datasets for estimation and evaluation, respectively. In each case, the size of the testing dataset is reported in parentheses. For the second method, our forecasting models are re-estimated based on the lag orders used in Table 3 for each quantile range.

Table 5
Forecast evaluations for the full samples.***, **

Models:	CAC 40	DAX 30	FTSE 100	NIKKEI 225	S&P 500
QAR Model	1.810	1.923	1.181	1.868	1.319
MS-GARCH(1,1)-N	2.088***	2.459***	1.319***	2.421***	1.295
MS-GARCH(1,1)-ST	2.259***	2.582***	1.350***	2.297***	1.477***
MS-GARCH(1,1)-SST	2.809***	2.997***	1.172	2.090***	2.872***
MS-GJRGARCH (1,1)-N	1.620	1.547	0.957	1.955***	0.947
MS-GJRGARCH (1,1)-ST	1.902***	1.777	0.831	1.891***	2.448***
MS-GJRGARCH (1,1)-SST	2.277***	2.231***	1.214***	2.051***	2.942***
Taylor 98	2.225***	2.401***	1.530***	2.306***	1.649***
Taylor 95	2.212***	2.393***	1.521***	2.295***	1.641***
Taylor 90	2.201***	2.382***	1.515***	2.288***	1.625***
Huang SD	2.189***	2.364***	1.501***	2.283***	1.612***
Huang WSD	2.172***	2.346***	1.481***	2.278***	1.589***
Huang MSD	2.182***	2.360***	1.494***	2.282***	1.609***

This table presents the MSEs of the volatility forecasts based on 1500 out-of-sample predictions. The left column lists the forecasting models benchmarked in this study. Apart from the QAR model proposed in the study, three variants each of the MS- GARCH(1,1) model and the MS- GJRGARCH (1,1) model, based on various distribution assumptions, are reported. N stands for the normal distribution, ST stands for the Student's t distribution, and SST stands for the skewed Student's distribution. Among the QR-based models, the models proposed by Taylor (2005) and Huang (2012) are tested. The symbolic outcomes of the Diebold-Mariano test comparing the results of both GARCH-based and quantile-based models to the QAR volatility prediction are given in parentheses. The two models being compared have equal predictive ability under the null.

*** Represent statistical significance at the 1% level, respectively.

** Represent statistical significance at the 5% level, respectively.

conditional quantiles. In contrast, there will be an increase in the right tail, i.e. $Q_{y_{t,\tau}}{}^{(1)} < Q_{y_{t,\tau}}{}^{(2)}$, as the autoregressive coefficients have a negative effect on the fitted conditional quantiles. Hence, the distribution of stock returns is stretched.

6. Conclusion

The QR framework of Koenker and Bassett Jr (1978) provides a means with which to model and analyse any time-varying distribution of interest. In this paper, we propose a novel method for forecasting financial assets' return volatility via combining QRs with Li et al.'s (2015) QPACF to identify the autoregressive dependence patterns in returns' series over a wide range of quantiles of the returns' distribution. Our first contribution concentrates on demonstrating that the quantile dependence pattern is variable across the returns' distribution. Using data derived from five stock indices, namely, the CAC 40, DAX 30, FTSE 100, NIKKEI 225, and S&P 500, our results show that the direction of the influence of past returns varies across the spectrum of quantiles of the returns' distribution. While the autoregressive coefficients are positive for quantiles close to the left tail, the opposite sign for these coefficients is obtained at the right end of the distribution. We find no significant dependence in quantiles corresponding to the middle section of the returns' distribution. Moreover, quantiles at the upper end of the quantile range exhibit higher lag order than those for the left tails (see Table 3). Additionally, the degree of persistence differs between the two tails, as the magnitudes of the significant coefficients for the extreme-right quantiles is greater than those observed for the left tail of the returns' distribution. This finding implies that the specification of an autoregressive forecasting model should change according to the section of the returns' distribution being forecast, as is the case with our QAR model.

The second key contribution of this work focuses on developing a

Table 6
Forecast evaluations for the sub-sample periods. This table presents the forecasting results for all the models for the three subsamples. Panel A shows the forecasting results the prior-crisis period, Panel B shows the forecasting results for the crisis period, and Panel C reports the forecasting results for the post-crisis period. *P*-values for the Diebold-Mariano test comparing the GARCH-based and quantile-based model predictions to the QAR volatility prediction are given in parentheses. *** and ** represents statistical significance at the 1% and 5% levels, respectively.

	CAC 40	DAX 30	FTSE 100	NIKKEI 225	S&P 500
Panel A: Forecasting evaluation for sub-sample (prior-crisis)					
QAR Model	2.093	2.520	1.200	1.988	1.343
MS-GARCH(1,1)-N	2.873 (***)	3.600 (***)	1.584 (***)	2.209 (***)	1.315
MS-GARCH(1,1)-ST	2.732 (***)	3.644 (***)	0.976	2.213 (***)	1.478 (***)
MS-GARCH(1,1)-SST	2.817 (***)	2.967 (***)	0.917	2.194 (***)	1.481 (***)
MS-GJRGARCH(1,1)-N	1.214	1.848	0.751	2.178 (***)	0.920
MS-GJRGARCH(1,1)-ST	1.229	1.828	0.613	2.157 (***)	0.879
MS-GJRGARCH(1,1)-SST	2.552 (***)	1.967	0.747	2.146 (***)	0.959
Taylor 98	2.505 2.501 2.502 2.493 2.490 2.481 (***)	2.966 (***)	1.464 (***)	2.249 (***)	1.545 (***)
Taylor 95	2.501 2.502 2.493 2.490 2.481 (***)	2.945 (***)	1.455 (***)	2.248 (***)	1.540 (***)
Taylor 90	2.502 (***)	2.941 (***)	1.459 (***)	2.249 (***)	1.530 (***)
Huang SD	2.493 (***)	2.932 (***)	1.422 (***)	2.245 (***)	1.516 (***)
Huang WSD	2.490 (***)	2.940 (***)	1.394 (***)	2.247 (***)	1.502 (***)
Huang MSD	2.481 (***)	2.925 (***)	1.403 (***)	2.245 (***)	1.515 (***)
Panel B: Forecasting evaluation for sub-sample (crisis)					
QAR Model	1.941	1.679	1.664	2.046	1.759
MS-GARCH(1,1)-N	5.188 (***)	4.306 (***)	8.199 (***)	3.264 (***)	10.015 (***)
MS-GARCH(1,1)-ST	5.411 (***)	7.294 (***)	8.783 (***)	3.309 (***)	14.413 (***)
MS-GARCH(1,1)-SST	7.490 (***)	11.922 (***)	14.786 (***)	3.077 (***)	14.643 (***)
MS-GJR-GARCH(1,1)-N	4.374 (***)	3.684 (***)	6.920 (***)	2.818 (***)	6.949 (***)
MS-GJR-GARCH(1,1)-ST	8.154 (***)	4.273 (***)	4.044 (***)	2.893 (***)	23.063 (***)
MS-GJR-GARCH(1,1)-SST	7.778 (***)	4.983 (***)	4.803 (***)	2.584 (***)	9.555 (***)
Taylor 98	2.887 (***)	3.235 (***)	2.477 (***)	2.303 (***)	2.815 (***)
Taylor 95	2.862 (***)	3.261 (***)	2.471 (***)	2.321 (***)	2.784 (***)
Taylor 90	2.840 (***)	3.243 (***)	2.463 (***)	2.325 (***)	2.775 (***)
Huang SD	2.882 (***)	3.299 (***)	2.474 (***)	2.372 (***)	2.899 (***)
Huang WSD	2.901 (***)	3.363 (***)	2.486 (***)	2.437 (***)	3.014 (***)
Huang MSD	2.900 (***)	3.309 (***)	2.487 (***)	2.396 (***)	2.966 (***)

Panel C: Forecasting evaluation for sub-sample (post-crisis)					
QAR Model	1.406	1.392	0.830	1.643	0.776
MS-GARCH(1,1)-N	1.424	1.302	0.838	2.222 (***)	0.744
MS-GARCH(1,1)-ST	1.501 (***)	1.455 (***)	1.147 (***)	2.615 (***)	0.890 (***)
MS-GARCH(1,1)-SST	1.952 (***)	2.063 (***)	0.840	2.298 (***)	1.115 (***)
MS-GJR-GARCH(1,1)-N	1.469 (***)	1.289	0.642	1.998 (***)	0.677
MS-GJR-GARCH(1,1)-ST	1.656 (***)	1.786 (***)	1.089 (***)	1.936 (***)	1.836 (***)
MS-GJR-GARCH(1,1)-SST	2.013 (***)	3.101 (***)	1.221 (***)	2.204 (***)	3.516 (***)
Taylor 98	1.699 (***)	1.655 (***)	0.956 (***)	1.996 (***)	0.935 (***)
Taylor 95	1.690 (***)	1.653 (***)	0.953 (***)	1.996 (***)	0.933 (***)
Taylor 90	1.682 (***)	1.646 (***)	0.949 (***)	1.989 (***)	0.931 (***)
Huang SD	1.673 (***)	1.642 (***)	0.946 (***)	1.982 (***)	0.928 (***)
Huang WSD	1.658 (***)	1.634 (***)	0.940 (***)	1.970 (***)	0.923 (***)
Huang MSD	1.668 (***)	1.640 (***)	0.944 (***)	1.979 (***)	0.927 (***)

QAR model framework suitable for volatility forecasting. We propose a volatility forecasting method that accommodates the quantile dependence in stock returns when generating conditional volatility forecasts. Using a battery of tests, we demonstrate that the QAR framework improves out-of-sample volatility forecasting significantly when compared with various MS-GARCH-type models and other quantile-based forecasting models. We observe that this outperformance is more pronounced during episodes of high volatility, such as the financial crisis of 2007–2009. We attribute the outperformance of our method to its ability to capture temporal variations in the returns' distribution by avoiding the distributional assumptions made by the GARCH-type models benchmarked in this paper. Being a quantile-based method, our model is able to forecast the full distribution of asset returns, thereby avoiding making assumptions about its distribution. Since our volatility forecasts are obtained by adopting a purely empirical approach, this approach is more flexible than those of other quantile-based methods, which, to some extent, employ a formulaic approach to obtaining volatility forecasts. The greater flexibility embedded in our method allows it to reproduce various structural features of the returns' distribution, resulting in improved forecasting performance.

As a third contribution, this paper illustrates the so called 'leverage effect' associated with conditional volatility by using the QAR model. This result provides further evidence to support the findings of related studies, such as Black (1976), Christie (1982), and Bekaert and Wu (2000). Although the economic utility of this stylized empirical fact is open to debate, our QAR model does provide a way to explain this phenomenon via QRs.

Our findings have implications for investors and policymakers. Our results suggest that the autoregression varies across the quantiles of the returns' distribution in terms of both magnitude and persistence, which sheds light on the predictive power of past returns based on the state of stock market. This insight could be useful for investors and policymakers who can adjust their trading strategies or portfolios according to different states of the stock market. Similarly, our model could act as an 'early warning system' for regulators to contain episodes of extreme volatility under high economic uncertainty.

In closing, we should point out some related issues beyond the scope of this study that could be relevant for future research. We have mentioned a few scenarios for which our method is relevant, but this aspect has not been elaborated upon. This study could, therefore, spawn future research that applies our method in situations other than those

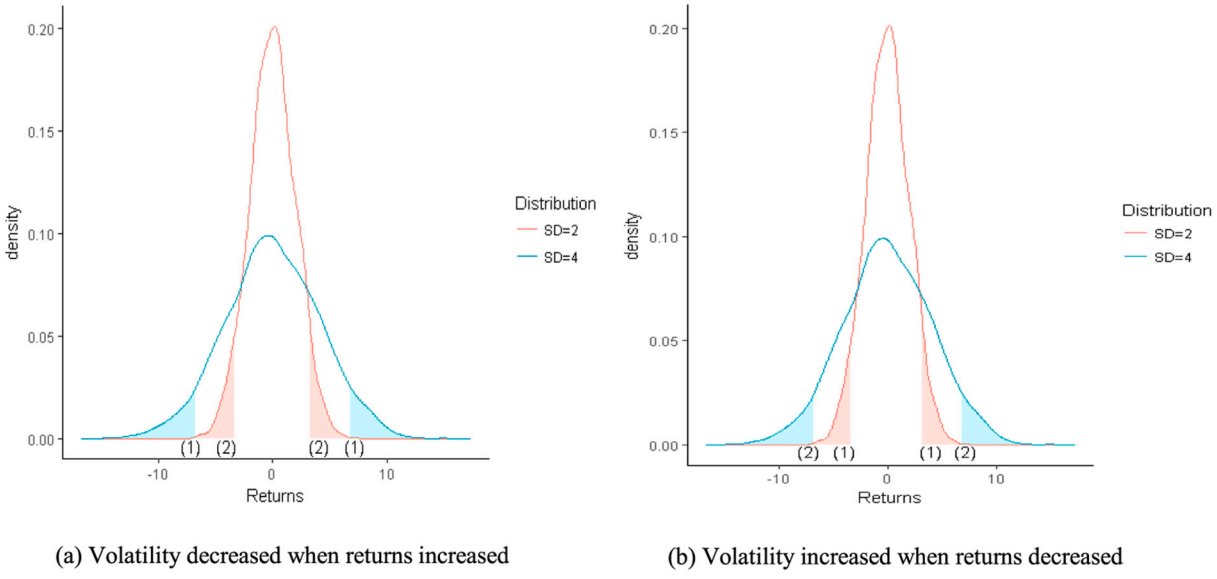

Fig. 7. "Leverage effects" of conditional volatility.
This figure shows the "leverage effects" of conditional volatility brought out by using quantile regression. In each plot, for illustration purposes, we use two curves (blue and red) to represent the distribution of stock returns for a financial market, where the blue density curve has a greater variance than the red one, but both curves have area τ. There are two possible scenarios with respect to the future direction of stock returns, i.e. increasing or decreasing stock returns. Based on the model in Table 2, we know that the coefficients have a positive effect on the fitted conditional quantiles in the left tail, while they have a negative effect in the right tail. In the left tail in plot (a), when there is an increase in stock returns in the future, i.e. $y_{t-1}^{(1)} < y_{t-1}^{(2)}$, there will be a corresponding increase in quantiles, i.e. $Q_{y_t,\tau}{}^{(1)} < Q_{y_t,\tau}{}^{(2)}$. To the contrary, owing to the negative autoregressive dependence present, there will be a decrease in fitted quantiles, i.e. $Q_{y_t,\tau}{}^{(1)} > Q_{y_t,\tau}{}^{(2)}$, in the right tail resulting in a contraction in the distribution of stock returns. Whereas, in the left tail in plot (b), when there is a decrease in future stock return, i.e. $y_{t-1}^{(1)} > y_{t-1}^{(2)}$, there will be a corresponding decrease in the fitted quantiles in the left tail, i.e. $Q_{y_t,\tau}{}^{(1)} > Q_{y_t,\tau}{}^{(2)}$. In the right tail, however, there will be an increase in the fitted quantiles, i.e. $Q_{y_t,\tau}{}^{(1)} < Q_{y_t,\tau}{}^{(2)}$, leading to the stretching of the distribution of stock returns.

presented in this paper. Second, our analysis does not examine variables other than the past returns, such as macroeconomic variables, which may influence the returns' distribution. Future research could remedy this shortcoming by including relevant variables, such as the economic growth rate or interest rates, in the analysis.

Acknowledgement

We gratefully acknowledge extremely helpful comments and suggestions from the two referees and the editor. We also benefited from discussions with participants at 2018 FMA European Conference in Norway, and seminars organized by the School of Management, Swansea University and Harbin Engineering University's Centre for Big Data and Business Intelligence. Additionally we thank Mike Adams for his insightful comments.

Author statement

The authors declare no conflict of interest. This paper was never published before and will not be sent to anywhere else for consideration of publication during the review process of this journal.

Appendix A. Appendix 1: The estimation of the sample QPACF

The estimation of $\varnothing_{kk,\tau}$ is given by:

$$\tilde{\varnothing}_{kk,\tau} = \frac{1}{\sqrt{(\tau-\tau^2)\tilde{\sigma}^2_{y|z}}} \cdot \frac{1}{n} \sum_{t=k+1}^{n} \psi_\tau \left(y_t - \tilde{\alpha}_{2,\tau} - \tilde{\beta}'_{2,\tau} \boldsymbol{z}_{t,k-1} \right) y_{t-k},$$

where:

$$\tilde{\sigma}^2_{y|z} = \frac{1}{n} \cdot \sum_{t=k+1}^{n} \left(y_{t-k} - \tilde{\alpha}_1 - \tilde{\beta}'_1 \boldsymbol{z}_{t,k-1} \right)^2,$$

$$\left(\tilde{\alpha}_1, \tilde{\beta}'_1 \right) = argmin_{\alpha,\beta} \sum_{t=k+1}^{n} (y_{t-k} - \alpha - \beta' z_{t,k-1})^2,$$

$$\left(\tilde{\alpha}_{2,\tau}, \tilde{\beta}'_{2,\tau} \right) = argmin_{\alpha,\beta} \sum_{t=k+1}^{n} \rho_\tau (y_t - \alpha - \beta' z_{t,k-1})$$

In traditional time series analyses, the first-order partial autocorrelation (PACF) is defined to be equal to the first-order autocorrelation. A similar approach is adopted in Li et al. (2015). Thus, the first-order quantile partial autocorrelation equals the first- order quantile autocorrelation, i.e. $\varnothing_{11,\tau} = qcor_\tau\{y_t, y_{t-1}\}$. Then, based on the definition of a quantile autocorrelation, we obtain:

$$\tilde{\varnothing}_{11,\tau} = \frac{1}{\sqrt{(\tau-\tau^2)\sigma^2_{y_{t-1}}}} \cdot \frac{1}{n} \cdot \sum_{t=2}^{n} \psi_\tau \left(y_t - Q_{\tau,y_t} \right) \left(y_{t-1} - E(y_{t-1}) \right),$$

where $Q_{\tau,\, y_t}$ is the τth unconditional quantile of y_t, i.e. $F(Q_{\tau,\, y_t}) = \tau$, and $F(\cdot)$ is the cumulative distribution function of y_t.

Next, we calculate the confidence bound for$\varnothing_{kk,\tau}$. As shown in Li et al. (2015), for a given $\tau \in (0,1)$, $\sqrt{n}\tilde{\varnothing}_{kk,\tau} \rightarrow_d N(0, \Omega_3(\tau,\tau))$. Thus, the confidence bound for $\widehat{\varnothing}_{kk,\tau}$ is $\pm 1.96\sqrt{\widehat{\Omega}_3/n}$,where

$$\widehat{\Omega}_3 = \frac{E[\psi_\tau(e_{t\tau})\psi(e_{t\tau})]\sum_{32}(\tau,\tau)}{\sqrt{(\tau-\tau^2)(\tau-\tau^2)}E\left(y_{t-k} - \alpha_1 - \beta'_1 z_{t,k-1}\right)^2},$$

A.1. and

$$e_{t\tau} = y_t - \phi_0(\tau) - \phi_1(\tau) y_{t-1} - \ldots - \phi_k(\tau) y_{t-k},$$

$$E[\psi_\tau(e_{t\tau})\psi(e_{t\tau})] = \frac{1}{n} \cdot \sum_{t=k+1}^{n} \psi_\tau(e_{t\tau})\psi_\tau(e_{t\tau}),$$

$$E\left(y_{t-k} - \alpha_1 - \beta'_1 z_{t,k-1}\right)^2 = \tilde{\sigma}^2_{y|z} = \frac{1}{n} \cdot \sum_{t=k+1}^{n} \left(y_{t-k} - \tilde{\alpha}_1 - \tilde{\beta}'_1 \boldsymbol{z}_{t,k-1} \right)^2,$$

$$\sum_{32}(\tau,\tau) = E\left(y_t^2\right) - 2A'_1(\tau)\sum_{31}^{-1}(\tau)A_0 + A'_1(\tau)\sum_{31}^{-1}(\tau)\Sigma_{30}\sum_{31}^{-1}(\tau)A_1(\tau)$$

In calculating the above equation for $\sum_{32}(\tau,\tau)$, as suggested by Li et al. (2015), we use the sample average to approximate $E(y_t^2)$, A_0, $A_1(\tau)$, Σ_{30}, and $\sum_{31}(\tau)$. Hence,

$$E\left(y_t^2\right) = \frac{1}{n} \cdot \sum_{t=k+1}^{n} y_t^2,$$

$$A_0 = E\left(y_{t-k} \boldsymbol{z}_{t,k-1}^{*}\right) = \frac{1}{n} \cdot \sum_{t=k+1}^{n} y_{t-k} \cdot (1, y_{t-1}, \ldots, y_{t-k+1})',$$

where

$$\boldsymbol{z}_{t,k-1}^{*} = \left(1, z_{t,k-1}'\right)' = (1, y_{t-1}, \ldots, y_{t-k+1})',$$

and

$$A_1(\tau) = E\left[f_{t-1}(0) y_{t-k} \boldsymbol{z}_{t,k-1}^{*}\right] = \frac{1}{n} \cdot \sum_{t=k+1}^{n} \cdot \tilde{f}_{t-1}(0) \cdot y_{t-k} \cdot (1, y_{t-1}, \ldots, y_{t-k+1})'$$

$$\Sigma_{30} = E\left[z_{t,k-1}^{*} z_{t,k-1}^{*\prime}\right] = \frac{1}{n} \cdot \sum_{t=k+1}^{n} (1, y_{t-1}, \ldots, y_{t-k+1})(1, y_{t-1}, \ldots, y_{t-k+1})'$$

$$\sum_{31}(\tau) = E\left[f_{t-1}(0) z_{t,k-1}^{*} z_{t,k-1}^{*\prime}\right]$$

$$= \frac{1}{n} \cdot \sum_{t=k+1}^{n} \cdot \tilde{f}_{t-1}(0) \cdot (1, y_{t-1}, \ldots, y_{t-k+1})(1, y_{t-1}, \ldots, y_{t-k+1})'$$

To evaluate $\tilde{f}_{t-1}(0)$ in the above equations, we adopt the method originally proposed by Hendricks and Koenker (1992), which is suggested by Li et al. (2015). That is, we let

$$\tilde{f}_{t-1}(0) = \frac{2h}{\tilde{Q}_{\tau+h}(y_t|F_{t-1}) - \tilde{Q}_{\tau-h}(y_t|F_{t-1})},$$

where h is referred to as the bandwidth, and $\tilde{Q}_{\tau}\left(y_t|F_{t-1}\right) = \tilde{\phi}_0(\tau) + \tilde{\phi}_1(\tau) y_{t-1} + \ldots + \tilde{\phi}_k(\tau) y_{t-k}$ is the estimated τth quantile of y_t. With respect to selecting the bandwidth, h, we let

$$h = n^{-\frac{1}{3}} z_{\alpha}^{\frac{2}{3}} \left\{ 1.5 \varnothing^2 \left(\Phi^{-1}(\tau) \right) \Big/ \left(2 \left(\Phi^{-1}(\tau) \right)^2 + 1 \right) \right\}^{1/3},$$

as suggested by Hall and Sheather (1988). Here, $\varnothing(\cdot)$ is the $N(0,1)$ probability density function, $\Phi(\cdot)$ is the$N(0,1)$ cumulative distribution function, and $z_{\alpha} = \Phi^{-1}\left(1 - \frac{\alpha}{2}\right)$. In order to construct the 95% confidence intervals, we set $\alpha = 0.05$ in our study.

Appendix B. Appendix 2: Robustness check

Forecast evaluation based on the Diebold-Mariano Test for 500 out-of-sample observations.

Model	CAC40	DAX30	FTSE100	NIKKEI225	S&P500
QAR Model	1.648	1.776	1.070	1.875	1.115
MS-GARCH(1,1)-N	1.737 (***)	2.058 (***)	1.096 (***)	2.151 (***)	0.867
MS-GARCH(1,1)-ST	1.720 (***)	1.756	1.101 (***)	2.206 (***)	1.121
MS-GARCH(1,1)-SST	2.013 (***)	1.768	0.962	2.332 (***)	2.213 (***)
MS-GJRGARCH(1,1)-N	1.594	1.343	0.787	2.006 (***)	1.103
MS-GJRGARCH(1,1)-ST	1.643	1.621	0.766	1.946 (***)	1.173 (***)
MS-GJRGARCH(1,1)-SST	1.843 (***)	2.306 (***)	0.983	2.123 (***)	2.119 (***)
Taylor 98	2.051 (***)	2.238 (***)	1.377 (***)	2.328 (***)	1.436 (***)
Taylor 95	2.034 (***)	2.230 (***)	1.369 (***)	2.315 (***)	1.427 (***)
Taylor 90	2.022 (***)	2.218 (***)	1.361 (***)	2.306 (***)	1.414 (***)
Huang SD	2.009 (***)	2.203 (***)	1.350 (***)	2.295 (***)	1.406 (***)

(continued on next page)

(*continued*)

Model	CAC40	DAX30	FTSE100	NIKKEI225	S&P500
Huang WSD	1.990	2.184	1.334	2.281	1.389
	(***)	(***)	(***)	(***)	(***)
Huang MSD	2.002	2.200	1.346	2.294	1.404
	(***)	(***)	(***)	(***)	(***)

Forecast evaluation based on the Diebold-Mariano Test for 1000 out-of-sample observations.

	CAC40	DAX30	FTSE100	NIKKEI225	S&P500
	CAC40	DAX30	FTSE100	NIKKEI225	S&P500
QAR Model	1.693	1.800	1.076	1.899	1.177
MS-GARCH(1,1)-N	1.680	2.300	1.186	2.356	1.116
		(***)	(***)	(***)	
MS-GARCH(1,1)-ST	2.047	2.563	1.033	2.245	1.203
	(***)	(***)		(***)	(***)
MS-GARCH(1,1)-SST	2.496	2.852	1.062	2.179	2.629
	(***)	(***)		(***)	(***)
MS-GJRGARCH(1,1)-N	1.429	1.355	0.835	1.969	1.197
				(***)	(**)
MS-GJRGARCH(1,1)-ST	1.483	1.854	0.797	1.933	2.237
		(***)		(***)	(***)
MS-GJRGARCH(1,1)-SST	1.849	2.343	0.970	2.107	2.925
	(***)	(***)		(***)	(***)
Taylor 98	2.113	2.296	1.410	2.358	1.534
	(***)	(***)	(***)	(***)	(***)
Taylor 95	2.106	2.290	1.405	2.352	1.525
	(***)	(***)	(***)	(***)	(***)
Taylor 90	2.098	2.281	1.400	2.346	1.512
	(***)	(***)	(***)	(***)	(***)
Huang SD	2.091	2.270	1.390	2.339	1.504
	(***)	(***)	(***)	(***)	(***)
Huang WSD	2.078	2.255	1.376	2.332	1.485
	(***)	(***)	(***)	(***)	(***)
Huang MSD	2.087	2.268	1.386	2.339	1.501
	(***)	(***)	(***)	(***)	(***)

Forecast evaluation based on the Diebold-Mariano Test for 2000 out-of-sample observations.

Model	CAC40	DAX30	FTSE100	NIKKEI225	S&P500
	CAC40	DAX30	FTSE100	NIKKEI225	S&P500
QAR Model	1.792	1.925	1.218	1.997	1.354
MS-GARCH(1,1)-N	2.103	3.038	1.387	2.450	1.412
	(***)	(***)	(***)	(***)	(***)
MS-GARCH(1,1)-ST	2.070	2.114	1.361	2.304	1.442
	(***)	(***)	(***)	(***)	(***)
MS-GARCH(1,1)-SST	2.805	3.368	1.149	2.045	2.105
	(***)	(***)		(***)	(***)
MS-GJRGARCH(1,1)-N	1.435	1.833	0.804	1.970	0.936
MS-GJRGARCH(1,1)-ST	1.936	1.786	1.128	1.949	0.924
	(***)				
MS-GJRGARCH(1,1)-SST	2.487	2.183	1.681	2.193	2.985
	(***)	(***)	(***)	(***)	(***)
Taylor 98	2.245	2.451	1.589	2.469	1.720
	(***)	(***)	(***)	(***)	(***)
Taylor 95	2.236	2.439	1.583	2.457	1.709
	(***)	(***)	(***)	(***)	(***)
Taylor 90	2.228	2.430	1.576	2.450	1.693
	(***)	(***)	(***)	(***)	(***)
Huang SD	2.218	2.413	1.561	2.443	1.680
	(***)	(***)	(***)	(***)	(***)
Huang WSD	2.204	2.396	1.537	2.437	1.653
	(***)	(***)	(***)	(***)	(***)
Huang MSD	2.213	2.408	1.553	2.442	1.675
	(***)	(***)	(***)	(***)	(***)

Appendix C. Appendix 3: In-sample estimation for the S&P 500 return series

This table reports the results of the quantile regression estimates over the full range of quantile levels for the S&P 500 return series for the sample period from 1 March 2000 to 13 March 2013 using 3268 observations. Each panel table reports the estimation results over a different range of quantile levels based on different lags for the AR terms. Note: The symbols ** and * indicate statistical significance at the 5% and 10% significance levels, respectively.

τ	0.01	0.02	0.03	0.04	0.05	0.06	0.07	0.08	0.09	0.10	0.11	0.12	0.13	0.14	0.15
Panel (a): Estimated parameters for $\tau \in (0.01,0.15)$															
Intercept	−3.866**	−2.991**	−2.626**	−2.317**	−2.093**	−1.891**	−1.761**	−1.620**	−1.541**	−1.439**	−1.346**	−1.259**	−1.180**	−1.125**	−1.054**
	(0.316)	(0.128)	(0.103)	(0.101)	(0.081)	(0.070)	(0.060)	(0.051)	(0.049)	(0.049)	(0.048)	(0.044)	(0.040)	(0.039)	(0.036)
SRLAG1	0.075	0.036	0.036	0.036	0.036	0.036	0.036	0.036	0.036	0.036	0.028	0.020	0.020	0.020	0.020
	(0.092)	(0.097)	(0.052)	(0.074)	(0.051)	(0.058)	(0.051)	(0.041)	(0.035)	(0.030)	(0.030)	(0.029)	(0.032)	(0.036)	(0.037)
SRLAG2	0.129	0.129**	0.111**	0.082*	0.082**	0.082**	0.082*	0.082*	0.081*	0.078*	0.078**	0.078**	0.070**	0.070**	0.070**
	(0.102)	(0.061)	(0.041)	(0.049)	(0.035)	(0.041)	(0.043)	(0.044)	(0.042)	(0.040)	(0.038)	(0.035)	(0.032)	(0.031)	(0.031)
SRLAG3	0.155**	0.153**	0.136**	0.136**	0.115**	0.115**	0.111**	0.111**	0.110**	0.110**	0.109**	0.109**	0.109**	0.109**	0.109**
	(0.079)	(0.069)	(0.048)	(0.039)	(0.040)	(0.047)	(0.041)	(0.031)	(0.029)	(0.032)	(0.035)	(0.036)	(0.038)	(0.038)	(0.037)
SRLAG4	0.153	0.113**	0.113**	0.113*	0.113**	0.111**	0.109**	0.096**	0.091**	0.091**	0.091**	0.091**	0.091**	0.085**	0.079**
	(0.102)	(0.049)	(0.028)	(0.060)	(0.040)	(0.038)	(0.037)	(0.033)	(0.030)	(0.030)	(0.030)	(0.030)	(0.031)	(0.030)	(0.027)
SRLAG5	0.019	0.019	0.019	0.019	0.019	0.038	0.044	0.044	0.044	0.051*	0.051*	0.051*	0.051	0.051	0.051
	(0.074)	(0.044)	(0.055)	(0.070)	(0.048)	(0.048)	(0.048)	(0.039)	(0.033)	(0.028)	(0.028)	(0.030)	(0.033)	(0.034)	(0.034)
Panel (b): Estimated parameters for $\tau \in (0.16,0.25)$															
	0.16	0.17	0.18	0.19	0.20	0.21	0.22	0.23	0.24	0.25	–	–	–	–	–
Intercept	−0.998**	−0.958**	−0.912**	−0.847**	−0.791**	−0.750**	−0.715**	−0.680**	−0.644**	−0.600**	–	–	–	–	–
	(0.035)	(0.035)	(0.034)	(0.033)	(0.032)	(0.031)	(0.031)	(0.030)	(0.030)	(0.030)	–	–	–	–	–
SRLAG1	0.006	0.006	0.006	0.006	0.004	0.004	0.002	−0.002	−0.002	−0.002	–	–	–	–	–
	(0.035)	(0.033)	(0.031)	(0.030)	(0.029)	(0.029)	(0.029)	(0.029)	(0.030)	(0.029)	–	–	–	–	–
SRLAG2	0.054*	0.054*	0.054**	0.054**	0.053**	0.050**	0.050*	0.050*	0.050*	0.052*	–	–	–	–	–
	(0.029)	(0.028)	(0.026)	(0.025)	(0.025)	(0.025)	(0.026)	(0.027)	(0.027)	(0.028)	–	–	–	–	–
SRLAG3	0.080**	0.076**	0.073**	0.077**	0.077**	0.078**	0.078**	0.078**	0.078**	0.078**	–	–	–	–	–
	(0.033)	(0.031)	(0.030)	(0.029)	(0.029)	(0.029)	(0.029)	(0.030)	(0.031)	(0.032)	–	–	–	–	–
SRLAG4	0.073**	0.073**	0.072**	0.069**	0.067**	0.067**	0.066**	0.066**	0.063**	0.061**	–	–	–	–	–
	(0.026)	(0.026)	(0.026)	(0.027)	(0.027)	(0.027)	(0.027)	(0.028)	(0.029)	(0.029)	–	–	–	–	–
Panel (c): Estimated parameters for $\tau \in (0.26,0.54)$															
	0.26	0.27	0.28	0.29	0.30	0.31	0.32	0.33	0.34	0.35	0.36	0.37	0.38	0.39	0.40
Intercept	−0.540**	−0.503**	−0.469**	−0.435**	−0.404**	−0.373**	−0.348**	−0.319**	−0.287**	−0.257**	−0.224**	−0.201**	−0.178**	−0.160**	−0.540**
	(0.028)	(0.027)	(0.027)	(0.026)	(0.025)	(0.024)	(0.024)	(0.023)	(0.022)	(0.022)	(0.021)	(0.021)	(0.020)	(0.020)	(0.028)
SRLAG1	−0.022	−0.023	−0.019	−0.021	−0.021	−0.017	−0.019	−0.022	−0.025	−0.028	−0.031	−0.033	−0.035	−0.037	−0.022*
	(0.023)	(0.023)	(0.024)	(0.024)	(0.024)	(0.025)	(0.025)	(0.024)	(0.023)	(0.023)	(0.022)	(0.022)	(0.022)	(0.022)	(0.023)
	0.41	0.42	0.43	0.44	0.45	0.46	0.47	0.48	0.49	0.50	0.51	0.52	0.53	0.54	–
Intercept	−0.121**	−0.104**	−0.076**	−0.054**	−0.032*	−0.009	0.011	0.029	0.047*	0.067**	0.083**	0.102**	0.117**	0.137**	–
	(0.019)	(0.019)	(0.019)	(0.019)	(0.018)	(0.018)	(0.018)	(0.018)	(0.018)	(0.018)	(0.018)	(0.018)	(0.018)	(0.018)	–
SRLAG1	−0.041*	−0.042**	−0.045**	−0.047**	−0.049**	−0.051**	−0.053**	−0.055**	−0.056**	−0.058**	−0.060**	−0.062**	−0.063**	−0.065**	–
	(0.021)	(0.021)	(0.021)	(0.021)	(0.021)	(0.021)	(0.021)	(0.021)	(0.021)	(0.021)	(0.021)	(0.021)	(0.021)	(0.021)	–
Panel (d): Estimated parameters for $\tau \in (0.55,0.75)$															
	0.55	0.56	0.57	0.58	0.59	0.60	0.61	0.62	0.63	0.64	0.65	0.66	0.67	0.68	0.69
Intercept	0.166**	0.183**	0.199**	0.222**	0.245**	0.265**	0.283**	0.304**	0.326**	0.349**	0.369**	0.390**	0.421**	0.438**	0.464**
	(0.018)	(0.018)	(0.018)	(0.018)	(0.018)	(0.018)	(0.018)	(0.018)	(0.018)	(0.019)	(0.019)	(0.019)	(0.020)	(0.020)	(0.020)
SRLAG1	−0.091**	−0.092**	−0.093**	−0.093**	−0.093**	−0.093**	−0.093**	−0.093**	−0.093**	−0.093**	−0.093**	−0.093**	−0.095**	−0.097**	−0.099**
	(0.018)	(0.018)	(0.018)	(0.018)	(0.018)	(0.018)	(0.018)	(0.018)	(0.018)	(0.019)	(0.019)	(0.019)	(0.020)	(0.020)	(0.020)
SRLAG2	−0.061**	−0.061**	−0.062**	−0.064**	−0.066**	−0.068**	−0.070**	−0.072**	−0.074**	−0.076**	−0.078**	−0.080**	−0.081**	−0.081**	−0.081**
	(0.027)	(0.027)	(0.027)	(0.026)	(0.026)	(0.026)	(0.026)	(0.026)	(0.026)	(0.025)	(0.025)	(0.025)	(0.025)	(0.025)	(0.025)
	0.70	0.71	0.72	0.73	0.74	0.75	–	–	–	–	–	–	–	–	–
Intercept	0.486**	0.505**	0.537**	0.558**	0.584**	0.615**	–	–	–	–	–	–	–	–	–
	(0.020)	(0.020)	(0.021)	(0.021)	(0.022)	(0.022)	–	–	–	–	–	–	–	–	–
SRLAG1	−0.100**	−0.101**	−0.101**	−0.102**	−0.102**	−0.104**	–	–	–	–	–	–	–	–	–
	(0.020)	(0.020)	(0.020)	(0.020)	(0.020)	(0.021)	–	–	–	–	–	–	–	–	–
SRLAG2	−0.083**	−0.083**	−0.086**	−0.087**	−0.090**	−0.090**	–	–	–	–	–	–	–	–	–
	(0.025)	(0.025)	(0.025)	(0.025)	(0.025)	(0.025)	–	–	–	–	–	–	–	–	–
Panel (e): Estimated parameters for $\tau \in (0.76,0.84)$															
	0.76	0.77	0.78	0.79	0.80	0.81	0.82	0.83	0.84	–	–	–	–	–	–
Intercept	0.663**	0.693**	0.726**	0.752**	0.803**	0.833**	0.873**	0.925**	0.957**	–	–	–	–	–	–
	(0.024)	(0.025)	(0.026)	(0.026)	(0.028)	(0.028)	(0.029)	(0.031)	(0.032)	–	–	–	–	–	–
SRLAG1	−0.126**	−0.126**	−0.129**	−0.130**	−0.132**	−0.132**	−0.132**	−0.136**	−0.136**	–	–	–	–	–	–
	(0.021)	(0.022)	(0.022)	(0.022)	(0.024)	(0.024)	(0.026)	(0.029)	(0.030)	–	–	–	–	–	–

(*continued on next page*)

(*continued*)

τ	0.01	0.02	0.03	0.04	0.05	0.06	0.07	0.08	0.09	0.10	0.11	0.12	0.13	0.14	0.15
SRLAG2	−0.124**	−0.126**	−0.127**	−0.127**	−0.128**	−0.131**	−0.134**	−0.134**	−0.134**	–	–	–	–	–	–
	(0.027)	(0.028)	(0.029)	(0.029)	(0.030)	(0.031)	(0.032)	(0.034)	(0.035)	–	–	–	–	–	–
SRLAG3	−0.033	−0.033	−0.033	−0.033	−0.033	−0.033	−0.034	−0.034	−0.035	–	–	–	–	–	–
	(0.033)	(0.033)	(0.033)	(0.032)	(0.031)	(0.030)	(0.029)	(0.028)	(0.027)	–	–	–	–	–	–
SRLAG4	−0.061**	−0.062**	−0.062**	−0.063**	−0.063**	−0.063**	−0.063**	−0.063**	−0.065**	–	–	–	–	–	–
	(0.023)	(0.024)	(0.024)	(0.024)	(0.025)	(0.025)	(0.025)	(0.027)	(0.027)	–	–	–	–	–	–
SRLAG5	−0.094**	−0.094**	−0.094**	−0.094**	−0.095**	−0.095**	−0.095**	−0.095**	−0.095**	–	–	–	–	–	–
	(0.024)	(0.024)	(0.023)	(0.023)	(0.023)	(0.023)	(0.023)	(0.023)	(0.024)	–	–	–	–	–	–
Panel (f): Estimated parameters for $\tau \in (0.85, 0.99)$															
	0.85	0.86	0.87	0.88	0.89	0.90	0.91	0.92	0.93	0.94	0.95	0.96	0.97	0.98	0.99
Intercept	1.030**	1.082**	1.152**	1.207**	1.278**	1.340**	1.422**	1.515**	1.616**	1.803**	1.933**	2.115**	2.364**	2.808**	3.555**
	(0.032)	(0.033)	(0.036)	(0.038)	(0.041)	(0.043)	(0.045)	(0.050)	(0.060)	(0.065)	(0.060)	(0.085)	(0.095)	(0.238)	(0.263)
SRLAG1	−0.201**	−0.201**	−0.201**	−0.204**	−0.211**	−0.217**	−0.218**	−0.218**	−0.227**	−0.229**	−0.229**	−0.229**	−0.229**	−0.229**	−0.229
	(0.029)	(0.027)	(0.026)	(0.027)	(0.032)	(0.034)	(0.038)	(0.041)	(0.043)	(0.030)	(0.027)	(0.041)	(0.050)	(0.111)	(0.155)
SRLAG2	−0.167**	−0.171**	−0.175**	−0.175**	−0.175**	−0.175**	−0.175**	−0.175**	−0.175**	−0.175**	−0.175**	−0.175**	−0.175**	−0.175*	−0.175**
	(0.031)	(0.031)	(0.032)	(0.033)	(0.035)	(0.035)	(0.034)	(0.034)	(0.037)	(0.039)	(0.032)	(0.035)	(0.040)	(0.092)	(0.061)
SRLAG3	−0.089**	−0.090**	−0.090**	−0.090**	−0.090**	−0.090**	−0.093**	−0.102**	−0.102**	−0.103**	−0.113**	−0.121**	−0.121**	−0.121	−0.121*
	(0.030)	(0.029)	(0.027)	(0.026)	(0.024)	(0.024)	(0.027)	(0.032)	(0.033)	(0.022)	(0.020)	(0.030)	(0.034)	(0.090)	(0.073)
SRLAG4	−0.108**	−0.108**	−0.110**	−0.112**	−0.112**	−0.112**	−0.116**	−0.116**	−0.116**	−0.130**	−0.130**	−0.130**	−0.130**	−0.145	−0.215**
	(0.028)	(0.028)	(0.027)	(0.027)	(0.028)	(0.028)	(0.030)	(0.034)	(0.039)	(0.030)	(0.034)	(0.042)	(0.055)	(0.109)	(0.051)
SRLAG5	−0.116**	−0.116**	−0.116**	−0.116**	−0.116**	−0.116**	−0.116**	−0.116**	−0.116**	−0.116**	−0.116**	−0.116**	−0.116**	−0.116	−0.116*
	(0.028)	(0.029)	(0.031)	(0.031)	(0.031)	(0.031)	(0.030)	(0.028)	(0.029)	(0.027)	(0.028)	(0.044)	(0.037)	(0.125)	(0.066)
SRLAG6	−0.088**	−0.088**	−0.088**	−0.088**	−0.088**	−0.088**	−0.088**	−0.088**	−0.088**	−0.088**	−0.088**	−0.088**	−0.088*	−0.088	−0.088
	(0.027)	(0.028)	(0.031)	(0.032)	(0.032)	(0.031)	(0.031)	(0.034)	(0.040)	(0.039)	(0.035)	(0.036)	(0.046)	(0.108)	(0.062)
SRLAG7	−0.090**	−0.090**	−0.090**	−0.090**	−0.090**	−0.090**	−0.090**	−0.090**	−0.090**	−0.090**	−0.090**	−0.090**	−0.100**	−0.100	−0.100
	(0.027)	(0.028)	(0.030)	(0.030)	(0.029)	(0.027)	(0.025)	(0.025)	(0.030)	(0.033)	(0.029)	(0.040)	(0.047)	(0.092)	(0.118)
SRLAG8	−0.106**	−0.106**	−0.106**	−0.106**	−0.106**	−0.106**	−0.106**	−0.106**	−0.106**	−0.106**	−0.108**	−0.117**	−0.130**	−0.157	−0.157**
	(0.030)	(0.032)	(0.035)	(0.036)	(0.037)	(0.037)	(0.037)	(0.038)	(0.039)	(0.028)	(0.030)	(0.034)	(0.024)	(0.102)	(0.053)
SRLAG9	−0.077**	−0.077**	−0.077**	−0.077**	−0.077**	−0.077**	−0.077**	−0.077**	−0.077**	−0.077**	−0.077**	−0.077	−0.077	−0.077	−0.077
	(0.029)	(0.028)	(0.026)	(0.025)	(0.026)	(0.027)	(0.029)	(0.030)	(0.029)	(0.024)	(0.024)	(0.042)	(0.060)	(0.095)	(0.086)

References

Aït-Sahalia, Y., Fan, J., Laeven, R. J., Wang, C. D., & Yang, X. (2017). Estimation of the continuous and discontinuous leverage effects. *Journal of the American Statistical Association, 112*(520), 1–15.

Andersen, T. G., & Bollerslev, T. (1998). Answering the skeptics: Yes, standard volatility models do provide accurate forecasts. *International Economic Review, 19*(4), 885–905.

Ardia, D., Bluteau, K., Boudt, K., Catania, L., Ghalanos, A., Peterson, B., & Trottier, D. A. (2019). Markov-switching GARCH models in R: the MSGARCH package. *Journal of Statistical Software, 91*(1), 1–38.

Azizpour, S., Giesecke, K., & Schwenkler, G. (2018). Exploring the sources of default clustering. *Journal of Financial Economics, 129*(1), 154–183.

Barnes, M. L., & Hughes, A. T. W. (2002, November). *A Quantile Regression Analysis of the Cross Section of Stock Market Returns*. Working paper 02–2. Boston: Federal Reserve Bank of. Retrieved from http://ssrn.com/abstract=458522.

Baur, D. G., & Dimpfl, T. (2017). Think Again: Volatility Asymmetry and Volatility Persistence. Consulted from doi:https://doi.org/10.2139/ssrn.2806970.

Baur, D. G., Dimpfl, T., & Jung, R. C. (2012). Stock return autocorrelations revisited: A quantile regression approach. *Journal of Empirical Finance, 19*(2), 254–265.

Bekaert, G., & Wu, G. (2000). Asymmetric volatility and risk in equity markets. *The Review of Financial Studies, 13*(1), 1–42.

Bernanke, B., & Gertler, M. (2000). *Monetary Policy and Asset Price Volatility*. NBER working paper 7559. Cambridge, MA: National Bureau of Economic Research.

Black, F. (1976). Studies of stock Price volatility changes. In *Proceedings of the 1976 Meetings of the American Statistical Association, Business and Economical Statistics Section* (p. 177). Washington, DC: American Statistical Association.

Bollerslev, T. (1986). Generalized autoregressive conditional heteroskedasticity. *Journal of Econometrics, 31*(3), 307–327.

Bondell, H. D., Reich, B. J., & Wang, H. (2010). Noncrossing quantile regression curve estimation. *Biometrika, 97*(4), 825–838.

Bouri, E., Jalkh, N., & Roubaud, D. (2019). Commodity volatility shocks and BRIC sovereign risk: A GARCH-quantile approach. *Resources Policy, 61*, 385–392.

Campbell, J. Y., & Hentschel, L. (1992). No news is good news: An asymmetric model of changing volatility in stock returns. *Review of Economic Studies, 31*(3), 281–318.

Carr, P., & Wu, L. (2017). Leverage effect, volatility feedback, and self-exciting market disruptions. *Journal of Financial and Quantitative Analysis, 52*(5), 2119–2156.

Choi, J. E., & Shin, D. W. (2018). Quantile forecasts for financial volatilities based on parametric and asymmetric models. *Journal of the Korean Statistical Society, 48*(1), 68–83.

Christie, A. A. (1982). The stochastic behavior of common stock variances: Value, leverage and interest rate effects. *Journal of Financial Economics, 10*(4), 407–432.

Demirgüç-Kunt, A., Feyen, E., & Levine, R. (2012). The evolving importance of banks and securities markets. *The World Bank Economic Review, 27*(3), 476–490.

Diebold, F. X., & Mariano, R. (1995). Comparing predictive accuracy. *Journal of Business and Economic Statistics, 13*(3), 253–265.

Dimpfl, T., & Baur, D. G. (2016). *Inter-Quantile Ranges and Volatility of Financial Data*. https://doi.org/10.2139/ssrn.2835951

Engle, R. F. (1982). Autoregressive conditional heteroscedasticity with estimates of the variance of United Kingdom inflation. *Econometrica, 50*(4), 987–1007.

Engle, R. F., & Manganelli, S. (2004). CAViaR: Conditional autoregressive value at risk by regression quantiles. *Journal of Business & Economic Statistics, 22*(4), 367–381.

Engle, R. F., & Ng, V. K. (1993). Measuring and testing the impact of news on volatility. *Journal of Finance, 48*(5), 1749–1778.

Engle, R. F., & Patton, A. J. (2001). What good is a volatility model?. Consulted from http://archive.nyu.edu/handle/2451/26881.

Fama, E. F. (1970). Efficient capital markets: A review of theory and empirical work. *Journal of Finance, 25*(2), 383–417.

Ferrando, L., Ferrer, R., & Jareño, F. (2017). Interest rate sensitivity of Spanish industries: A quantile regression approach. *The Manchester School, 85*(2), 212–242.

Glosten, L. R., Jagannathan, R., & Runkle, D. E. (1993). On the relation between the expected value and the volatility of the nominal excess return on stocks. *The Journal of Finance, 48*(5), 1779–1801.

Gong, X., & Lin, B. (2018). Structural breaks and volatility forecasting in the copper futures market. *Journal of Futures Markets, 38*, 290–339.

Haas, M., Mittnik, S., & Paolella, M. S. (2004). A new approach to Markov-switching GARCH models. *Journal of Financial Econometrics, 2*(4), 493–530.

Hall, P., & Sheather, S. J. (1988). On the distribution of a studentized quantile. *Journal of the Royal Statistical Society Series B, 50*, 381–391.

Han, H., Linton, O., Oka, T., & &Whang Y. J.. (2016). The cross-quantilogram: Measuring quantile dependence and testing directional predictability between time series. *Journal of Econometrics, 193*(1), 251–270.

Hendricks, W., & Koenker, R. (1992). Hierarchical spline models for conditional quantiles and the demand for electricity. *Journal of the American Statistical Association, 87*, 58–68.

Huang, A. Y. (2012). Volatility forecasting by quantile regression. *Applied Economics, 44*(4), 423–433.

Kannadhasan, M., & Das, D. (2020). Do Asian emerging stock markets react to international economic policy uncertainty and geopolitical risk alike? A quantile regression approach. *Finance Research Letters, 34*. https://doi.org/10.1016/j.frl.2019.08.024

Kastner, G. (2016). Dealing with stochastic volatility in time series using the R package stochvol. *Journal of Statistical Software, 69*(5), 1–30.

Koenker, R., & Bassett, G., Jr. (1978). Regression quantiles. *Econometrica, 46*(1), 33–50.

Li, G., Li, Y., & Tsai, C. L. (2015). Quantile correlations and quantile autoregressive modeling. *Journal of the American Statistical Association, 110*(509), 246–261.

Ma, L., & Pohlman, L. (2008). Return forecasts and optimal portfolio construction: A quantile regression approach. *The European Journal of Finance, 14*(5), 409–425.

Meligkotsidou, L., Vrontos, I. D., & Vrontos, S. D. (2009). Quantile regression analysis of hedge fund strategies. *Journal of Empirical Finance, 16*(2), 264–279.

Nelson, D. B. (1991). Conditional heteroskedasticity in asset returns: A new approach. *Econometrica, 59*(2), 347–370.

Pearson, E. S., & Tukey, J. W. (1965). Approximate means and standard deviations based on distances between percentage points of frequency curves. *Biometrika, 52*(3/4), 533–546.

Pires, P., Pereira, J. P., & Martins, L. F. (2015). The empirical determinants of credit default swap spreads: A quantile regression approach. *European Financial Management, 21*(3), 556–589.

Poon, S. H., & Granger, C. W. (2003). Forecasting volatility in financial markets: A review. *Journal of Economic Literature, 41*(2), 478–539.

Shephard, N., & Sheppard, K. (2010). Realising the future: Forecasting with high-frequency-based volatility (heavy) models. *Journal of Applied Econometrics, 25*(2), 197–231.

Sim, N., & Zhou, H. (2015). Oil prices, US stock return, and the dependence between their quantiles. *Journal of Banking & Finance, 55*, 1–8.

Taylor, J. W. (2005). Generating volatility forecasts from value at risk estimates. *Management Science, 51*(5), 712–725.

Trapin, L. (2017). Can volatility models explain extreme events? *Journal of Financial Econometrics, 16*(2), 297–315.

Troster, V., Bouri, E., & Roubaud, D. (2019). A quantile regression analysis of fights-to-safety with implied volatilities. *Resources Policy, 62*, 482–495.

Veronesi, P. (1999). Stock market overreactions to bad news in good times: A rational expectations equilibrium model. *The Review of Financial Studies, 12*(5), 975–1007.

Wang, X., Shrestha, K., & Sun, Q. (2019). Forecasting realized volatility: A Markov switching approach with time-varying transition probabilities. *Accounting and Finance, 59*, 1947–1975.

Xiao, J., Hu, C., Ouyang, G., & Wen, F. (2019). Impacts of oil implied volatility shocks on stock implied volatility in China: Empirical evidence from a quantile regression approach. *Energy Economics, 80*, 297–309.

Zhang, Y., Lei, L., & Wei, Y. (2020). Forecasting the Chinese stock market volatility with international market volatilities: The role of regime switching. *North American Journal of Economics and Finance, 52*. https://doi.org/10.1016/j.najef.2020.101145

Zhang, Y., Ma, F., & Wei, Y. (2019). Out-of-sample prediction of the oil futures market volatility: A comparison of new and traditional combination approaches. *Energy Economics, 81*, 1109–1120.

Žikeš, F., & Baruník, J. (2016). Semi-parametric conditional quantile models for financial returns and realized volatility. *Journal of Financial Econometrics, 14*(1), 185–226.